21

Magnetospheric Interactions with Satellites

Margaret G. Kivelson
IGPP and Dept. of Earth & Space Sciences, University of California, Los Angeles

Fran Bagenal
LASP and Dept. of Astrophysical & Planetary Sciences, University of Colorado

William S. Kurth
Department of Physics and Astronomy, University of Iowa

Fritz M. Neubauer
Institut für Geophysik und Meteorologie, Universität zu Köln

Chris Paranicas, Joachim Saur
The Johns Hopkins University Applied Physics Laboratory

21.1 INTRODUCTION

The Galilean moons of Jupiter, Io, Europa, Ganymede and Callisto are embedded within the magnetospheric plasma that approximately corotates with Jupiter – that is, the plasma circles the planet at close to Jupiter's 10-hour spin period. The azimuthal speed of the plasma at the orbits of the Galilean moons is faster than the orbital velocity of the moons, so the plasma flows over the moons from their trailing hemispheres and sweeps ahead of them in their orbital motion. (Relevant properties of the plasma conditions near the satellites are provided in Table 21.1 while properties of the moons are provided in the book Appendix 2.)

When a flowing fluid such as water or air encounters an obstacle, it changes its course and a region of disturbance develops. The flow upstream and to the sides of the obstacle is perturbed (as in the bow wave of a moving ship), the disturbance often extending quite far downstream (in the wake). The precise features of the region of modified flow depend on the size and nature of the obstacle and the properties of the fluid (see Table 21.1), such as the ratio of the relative flow velocity to the velocity of waves in the fluid rest system (the Mach number), or the ratio, R, of a characteristic length, L, times a velocity, u, to the kinematic viscosity of the fluid ($R = Lu/\nu$ where ν is kinematic viscosity whose units are $m^2\ s^{-1}$). Examples of these statements come from common experience. Flow disturbances differ greatly in low viscosity fluids like water and high viscosity fluids like molasses. Ships and planes are streamlined to reduce turbulent flow in the wake but even a well-designed jet plane creates a shock when it travels faster than the speed of sound in air. In electrically conducting and magnetized plasmas such as those found in the jovian magnetosphere, the range of properties that must be considered is more extensive than in a fluid such as air or water. One must consider the electromagnetic properties of the plasma, and also such properties of the moons as their internally generated magnetic fields, their electrical conductivity on the global scale, the rate at which they lose neutral molecules and atoms that can be ionized in their surroundings, and the effects of currents that couple them to the jovian ionosphere.

The interactions of the moons with the flowing magnetospheric plasma are in some ways analogous to the interactions of the planets and other bodies with the flowing solar wind. The analogy cannot be pushed too far, but it is helpful in revealing how the geophysical characteristics of a planet modify the interaction.

Earth provides a well-studied example of the interaction of the solar wind with a magnetized planet. The planetary magnetic field stands off and deflects the solar wind far above the surface, forming the cavity within the solar wind – the magnetosphere. The boundary of a magnetosphere is the magnetopause, and within this boundary magnetic field lines have either one or two ends on the planet.

Venus, an unmagnetized planet with an electrically conducting ionosphere enwrapping its dense atmosphere, responds differently from the magnetized planets. Slowing and deflection of the shocked solar wind result from currents that flow through Venus's ionosphere and into the solar wind above a boundary referred to as the ionopause (Luhmann 1995). Solar wind field lines draped around the planet form an extended planetary tail. Neutral atoms from the atmosphere escape into the solar wind where they can be ionized and thus, "mass-load" the incident solar wind. Comets, though small bodies, are enveloped by clouds of neutrals and ions that fill a volume many times larger than the source body. The cometary interaction with the solar wind is dominated by the effects of mass loading.

An example of a different type of interaction is provided by Earth's moon, which spends part of every month in the solar wind. The Moon has neither an atmosphere/ionosphere nor a large-scale magnetic field and is a poor conductor of electrical current. Currents do not couple the Moon to the incident solar wind. Instead, the solar wind flows virtually unimpeded on to the upstream surface of the Moon where charged particles are absorbed, thereby creating a void in the solar wind over a limited region downstream (Luhmann 1995).

One significant element of the interaction between the solar wind and the planets that has not been observed in the vicinity of the Galilean moons is a shock bounding the upstream interaction region. In the solar wind, shocks develop because the plasma flows at velocities far higher than the group velocities of the magnetohydrodynamic (MHD) waves that transmit large-scale perturbations in a magnetized plasma, meaning that the relative velocity is "supersonic" in a generalized sense. Downstream of the shocks, the flow velocity drops below the fastest MHD wave velocity. In contrast, near the Galilean moons, MHD waves can transport energy and momentum faster than the relative speed of Jupiter's magnetospheric plasma, so the fastest MHD waves can propagate upstream of a moon, perturbations that slow and divert the flow develop gradually, and shocks do not form except possibly at Callisto.

This brief overview of planetary interaction regions suggests that the interactions of the moons of Jupiter with the plasma that flows by them should differ for bodies with or without an internal magnetic field, and should depend on the electrical conductivity of the moon's ionosphere and the presence of neutrals that may be sources of local mass loading and elastic and inelastic collisions, particularly at Io. As we introduce the individual moons, we pay special attention to these possibilities.

21.2 PROPERTIES OF THE GALILEAN MOONS

The four major moons of Jupiter range in size from Europa (radius 1560 km, slightly smaller than Earth's moon) to Ganymede (radius 2634 km, similar in size to Mercury). Their orbits lie deep within the jovian magnetopause, which stands well above the surface of Jupiter, typically by 60–100 R_J (R_J = 71 492 km) along the Jupiter–Sun direction (Joy *et al.* 2002). The densities of the moons (see Appendix 2) decrease with radial distance from Jupiter because of the increasing fraction of icy volatile materials that they contain. Io is ice-free, Europa has a thin (~100 km) ice crust, Ganymede has a thick (~800 km) ice crust, and Callisto is ice-rich throughout its interior (see Chapter 13). Io has an atmosphere and an ionosphere; there is some evidence that the atmosphere is patchy with increased density near the volcanic plumes and possibly above other hot spots on the surface. Neutral atmospheres or coronae are present around the other moons (see Chapter 19). The atmospheres are not necessarily bound, but there is evidence that on Io (Lellouch *et al.* 1990), Europa, and Ganymede (Hall *et al.* 1998) the exobase (the surface below which the atmosphere is collision-dominated) is above the surface. Very little is known directly about Callisto's thin atmosphere, whose presence can be inferred from the carbon dioxide characteristics in surface spectra and radio science electron profiles (Kliore *et al.* 2000).

21.2.1 Internal Magnetic Fields

An important objective of the *Galileo* mission was to establish the properties of the internal magnetic fields of the Galilean moons. Quite unexpectedly, Ganymede was found to have a permanent dipole moment with equatorial field magnitude of 719 nT (Kivelson *et al.* 2002). This field was interpreted as dynamo-driven implying that, as for Earth, there is conducting fluid in the deep interior whose motions generate the observed dipole moment.

Internal magnetic fields can arise from sources other than dynamo action. For example, an induced magnetic field can arise if currents are driven in a conducting layer within a planet by a periodically changing magnetic field. Indeed, a periodically varying external field is present at the positions of the Galilean moons. All of their orbits lie very close to Jupiter's rotational equatorial plane. Because Jupiter's dipole moment is tilted by about 10° relative to its rotation axis and because of the local time dependence of the current encircling Jupiter in the near equatorial plasma sheet (Khurana 2001), the orientation of Jupiter's magnetospheric field at the locations of the moons changes periodically. The field is dominantly southward at the satellites at all times, but the signs of the radial and azimuthal components change each jovian rotation period. Thus the external fields include a periodic contribution in the plane perpendicular to Jupiter's spin axis. We will refer to this periodically varying portion of the background field as the driving field.

Because the driving field is approximately uniform over the scale size of a moon, it has the symmetry of the Legendre polynomial of order 0, requiring the symmetry of the induced field to be approximately dipolar. The induced dipole's axis lies in the moon's equatorial plane and its magnitude and direction change at the synodic period of Jupiter. (The synodic period describes the apparent period of Jupiter's rotation observed from a body in orbit around it.) If the moon's conducting layer is deeply buried, the field at the surface of the moon will be very small compared with the driving field, but if the conducting layer is a shell relatively near the surface, a time-varying dipole moment may have a maximum surface magnitude equal to the maximum value of the driving field. Internal fields of this type have been found at Europa, Callisto, and Ganymede (Kivelson *et al.* 1999, 2002) and we will later discuss the effects of induced fields on the plasma interactions. The ratio of the maximum field arising from internal sources ($B_{\rm int}^{\rm surf}$) to the background external field ($B_{\rm bg}$) at the orbits of the moons is tabulated in Table 21.2.

21.2.2 Neutral Sources

The Galilean moons are significant sources of neutral gases (further discussed in Chapter 23). The first evidence was obtained from the observation of a cloud of neutral sodium that moves with Io around its orbit (Brown 1974, Smyth and McElroy 1977). The neutral sodium spreads into a disk hundreds of R_J across (Mendillo *et al.* 1990). Brown *et al.*

(1983) summarize the evidence that sodium (easily observed spectroscopically) is a minor constituent of the neutral material escaping Io. The dominant neutrals are sulfur and oxygen, mostly likely in the form of sulfur dioxide (SO_2), which readily dissociates to give O and S. The neutrals are ionized by processes including photoionization, electron impact ionization, and charge exchange, thereby adding heavy ions to the magnetosphere, where they spread out into an extended structure referred to as the Io plasma torus (see Chapter 23). The rate at which neutral material is added to the magnetosphere is roughly one ton per second (Hill *et al.* 1983). The newly ionized neutrals are referred to as pickup ions because as soon as they are ionized, they are accelerated to the speed of the bulk plasma flow.

The moons other than Io also serve as neutral sources, although at a much-reduced rate. Most of the neutral sources have not been observed directly, but their presence has been inferred from measurements of newly ionized neutrals as we discuss in Section 21.4.3.

21.2.3 Sputtering as a Source of Neutrals and Ions

Surface sputtering refers to the liberation of neutrals by the action of incident ions or electrons. In Chapter 20, Johnson *et al.* describe the physical alterations to a surface by charged particle radiation. Once a neutral atom or molecule is sputtered from the surface it may fall back to another part of the surface, enter a bound orbit of the satellite, or escape. For a uniformly volatile surface, sputtering should redistribute material away from regions that receive the highest levels of incident charged particle flux. Several researchers have estimated the global sputtering rates at the satellites, assuming all surface points receive equal flux (see, for instance, Cooper *et al.* (2001)). These calculations convolve particle intensities with yields, the number of neutrals freed per incident ion. Johnson has compiled yield data for the sputtering of icy surfaces (Chapter 20, Johnson 1990), including a number of target materials. His work emphasizes that it is the electronic excitations by MeV-energy ions, not the nuclear collisions, that produce the highest yields.

Sputtering data have been used to estimate the rate of erosion at Ganymede's polar caps. Erosion at the rate of $\sim$8 m Gyr^{-1} would occur if neutrals were not redistributed on the surface (Paranicas *et al.* 1999). At the satellites other than Ganymede, sputtering estimates have to this time ignored aspects of the satellite electrodynamics. For example, plasma flow diverted around satellites reduces the sputtering rates and this has consequences for how quickly satellites are resurfaced. A sophisticated analysis of the focusing and shielding effects of satellite fields may suggest preferred sputtering locations, which could provide interpretations of surface features detected remotely. Surface sputtering also serves as a prime source of the neutral atmospheres.

21.2.4 Atmosphere and Ionosphere

As contrasted with Earth's moon, the Galilean moons have atmospheres above all or much of their surfaces. Ionospheres form within the atmospheres through the mechanisms of electron impact ionization and photoionization and these ionospheres contribute in a crucial way to the plasma interactions. The ionospheres are electrically conductive and thus carry part of a current system that is continued outside the ionosphere by plasma currents, to be discussed below. The properties of the ionospheric currents are usually described in terms of the electrical conductivity of the ionosphere. Because a strong background magnetic field threads the ionospheres, the conductivities are strongly anisotropic. In the direction of the magnetic field, the conductivity is referred to as the *parallel* or *Birkeland* conductivity. The Birkeland conductivity is so high that it short-circuits the field-aligned component of the ionospheric electric field, and normally electrical equipotentials align with the ionospheric magnetic field lines. Perpendicular to the magnetic field direction, the conductivity has components parallel to the electric field (*Pedersen* conductivity) and perpendicular to the electric field (*Hall* conductivity).

Because the electric field vanishes in the field-aligned direction through the ionosphere, it is meaningful to integrate the transverse Pedersen and Hall conductivities along the magnetic field direction to evaluate the Pedersen and Hall conductances Σ_P and Σ_H, respectively (for a mathematical definition see Chapter 22). The forces that act on a flux tube in a moon's ionosphere can be expressed in terms of these conductances and the force balance expressions can consequently be used to derive other properties of the ionospheric flow such as its velocity.

The atmospheres within which the ionospheres form may be produced through surface warming, generally greatest on the illuminated or day side at low latitudes, but also present in hot spots on Io, and/or by sputtering. The non-uniform distribution of the atmospheres around the surfaces produces non-uniform ionospheres, and this affects the distribution of currents. On Io, patchiness is also associated with the volcanic plumes, which are localized sources of denser atmosphere. The effect of the non-uniform conductivity has been has been considered theoretically (Neubauer 1998b, 1999b) and observed on polar passes at Io (Kivelson *et al.* 2001b). The consequences are discussed in Chapter 22.

Mass loading contributes to the electrodynamics of the plasma interaction in ways that are analogous to the contributions of the ionospheric conductivities. Pickup ionization conserves momentum. An increase of the ion density results in a reduction of the flow velocity and its associated electric field. Thus, in developing the theory of the interaction, pickup effects can be directly incorporated into the above conductances (Neubauer 1998b, Saur *et al.* 1999) and the interaction region extends well above the atmospheric exobase.

The Pedersen current (aligned with the electric field) exerts forces that slow the flow in the ionosphere. The Hall current flows perpendicular to the electric and magnetic field, thereby breaking the symmetry of the interaction. The Hall current results in a rotation of the flow away from the corotation direction and produces ionospheric asymmetries (Saur *et al.* 1999), discussed in Chapter 22.

Table 21.1. Physical properties of the Galilean satellites and surrounding plasma.

Symbol (units), Physical property	Io	Europa	Ganymede	Callisto	Ref
Plasma and field parameters of the ambient magnetospheric plasma					
B_o(nT), jovian magnetic field, av. min (max)	1720 (2080)	370 (460)	64 (113)	4 (42)	1
n_e(elns cm^{-3}), Eq. av. (range) eln. density	2500 (1200–3800)	200 (18–250)	5 (1–10)	0.15 (0.01–0.70)	2
$< Z >$, Eq. av. (lobe) ion charge	1.3 (1.3)	1.5 (1.5)	1.3 (1)	1.5 (1)	3
$< A >$, Eq. av. (lobe) ion mass in m_p	22 (19)	18.5 (17)	14 (2)	16 (2)	3
n_i(ions cm^{-3}), av. (range) ion no. density	1920 (960–2900)	130 (12–170)	4 (1–8)	0.10 (0.01–0.5)	3
ρ_m(amu cm^{-3}), av. (range) ion mass density	42 300 (18 000–64 300)	2500 (200–3000)	54 (2–100)	1.6 (0.02–7)	3
kT_i (eV), equator (range) ion temperature	70 (20–90)	100 (50–400)	60 (10–100)	60 (10–100)	3
kT_e(eV), electron temperature	6	100	300	500	4
$p_{i,th}$(nPa), Eq. (range) pressure thermal plasma	22 (3–42)	2.1 (0.10–11)	0.04 (0.002–0.12)	0.001 (0.00–0.01)	3
$p_{i,cn}$(nPa) (20 keV–100 MeV ions)	10	12	3.6	0.37	5
p_e(nPa) (both "cold" and "hot" electrons)	2.4	3.2	0.2	0.01	
p(nPa), Eq. (max) total pressure	34 (54)	17 (26)	3.8 (3.9)	0.38 (0.39)	3, 5
v_{cr}(km s^{-1}), local corotation velocity	74	117	187	328	6
v_s(km s^{-1}), satellite orbit velocity	17	14	11	8	6
v_ϕ(km s^{-1})s plasma azimuthal vel. (range)	74 (70–74)	90 (70–100)	150 (95–163)	200 (130–280)	7
u(km s^{-1}), relative velocity (range), $v_\phi t$ v_s	57 (53–57)	76 (56–86)	139 (84–152)	192 (122–272)	
v_A(km s^{-1}), Eq. (range) Alfvén speed	180 (150–340)	160 (145–700)	190 (130–1700)	70 (30–6500)	8
c_s(km s^{-1}), Eq. (range) sound speed	29 (27–53)	92 (76–330)	280 (190–1400)	500 (230–4400)	9
$B_o^2/2\mu_o$(nPa), Eq. (lobe) magnetic pressure	1200 (1700)	54 (84)	1.6 (5)	0.006 (0.7)	1
ρu^2(nPa), Eq. av. (max) ram pressure	230 (350)	24 (38)	1.7 (4.1)	0.10 (0.90)	
ρu^2(nPa), lobe ram pressure	100	2.5	0.08	0.002	

1. B_o values are from (Khurana 1997).
2. Ranges in values of n_e come from *Voyager*-based models (Bagenal 1994) and from in situ measurements of Gurnett *et al.* (1996b, 2001) for Io, of Gurnett *et al.* (1998) and Kurth *et al.* (2001) for Europa, and of Gurnett *et al.* (2000) for Callisto (but see Section 23.3.1. for discussion of variability).
3. Thermal plasma estimates are based on *Voyager* in situ measurements in McNutt *et al.* (1981) and Bagenal (1994) as well as *Galileo* measurements reported by Crary *et al.* (1998), Frank and Paterson (2001b) and Paterson *et al.* (1999).
4. Effective electron temperatures (combining thermal and superthermal components) are interpolated from Scudder *et al.* (1981) and are consistent with Paterson *et al.* (1999), Frank and Paterson (2000, 2001b).
5. Values for pressure of ions >30 keV taken from from Mauk *et al.* (1996) and B. Mauk (personal communication, 2002) for Ganymede, from B. Mauk (personal communication, 2002) for Callisto. Values for Europa are from Paranicas *et al.* (2002). Values for the *Galileo* epoch differ by as much as a factor of 4 from *Voyager* values (Mauk *et al.* 1998). Pressure estimates for energetic particles assume composition is protons + oxygen + sulfur over the energy range 20 keV to 100 MeV.
6. The data for L_s , ρ_s, T_s, p_s, v_{cr}, and v_s, were taken from Morrison and Samz (1980).
7. v_ϕ estimates are the largest reported, likely to reflect the unperturbed flow speeds at the orbits of the moons. Lower values are also observed, especially close to the moons. The range of cited values are based on spectroscopic measurements (Brown 1994, Thomas *et al.* 2001) as well as in situ measurements from Hinson *et al.* (1998) and Frank and Paterson (2001a) for Io, from Paranicas *et al.* (2000) for Europa, from Williams (2001) for Ganymede, and from Kane *et al.* (1999) for Callisto. Krupp *et al.* (2001) report that at Europa's orbit, the flow speed is 20–80% of rigid corotation with large local time variations.
8. Estimates of v_A were made by employing density values from footnote 3 and B estimates from footnote 1.
9. For calculations of c_s, p is the total pressure and the average ion mass from footnote 3.

21.3 THE FIELD, PLASMA, AND RADIATION ENVIRONMENT

In the inner magnetosphere, the region in which the magnetic field (**B**) of Jupiter exceeds the fields arising from external currents, the magnetic energy dominates the energy density (Smith *et al.* 1976). The orbits of Io, Europa, and Ganymede are located in this region. Beyond about 20 R_J – the middle magnetosphere – a significant portion of the energy density resides in the thermal plasma and energetic particles that rotate around Jupiter and external currents produce a disk-like magnetic field structure. Callisto's orbit at 25 R_J lies in this region.

Properties of the magnetosphere that affect the plasma interactions are summarized in Table 21.1 in which many of the symbols are defined. The parameters $v_A \approx B(\mu_o m_i n_i)^{-1/2}$ and $c_s = (\gamma p/m_i n_i)^{1/2}$, where B is the magnetic field, m_i is the average ion mass, n_i is the ion number density, p is the thermal pressure, and γ is the ratio of specific heats, refer respectively to the Alfvén speed and the sound speed. These speeds determine the phase and group velocities of the three MHD waves.

The interaction between the plasma and a moon is strongly affected by properties of MHD waves, so some of their properties must be considered (Kivelson 1995). There are three independent wave modes that propagate at different speeds in different directions relative to the magnetic field direction. They are referred to as slow, intermediate, and fast, the designations alluding to the relative magnitudes of their phase and group velocities. For example, the MHD fast mode propagates across the magnetic field with a speed of $(v_A^2 + c_s^2)^{1/2}$. The slow mode propagates along the background field at close to the slower of the two wave

Table 21.1 – *continued* Physical properties of the Galilean satellites and surrounding plasma.

Symbol (units), Physical property	Io	Europa	Ganymede	Callisto	Ref
Characteristic parameters of the interaction					
B_s(nT), maximum satellite surface field	<50	<50	1500	<40	10
$\Sigma_A(S) = (\mu_o v_A)^{-1}$, Alfvén cond. Eq. (range)	4.4 (2.4–5.4)	4.9 (1.1–5.5)	4.2 (0.5–6)	12(0.1–25)	
Σ_P(S), av. (max) ionosph. Pedersen cond	~200	~30	2	~1000	11
Σ_H(S), av. (max) ionosph. Hall cond	100–200 (1200)	~10	0.1	~<10000	11
$\dot{M}/m_i(s^{-1})$, ions per s added locally to flow	$\sim 10^{28}$	$<6 \times 10^{26}$	$<6 \times 10^{26}$	$<5 \times 10^{25}$	12
Characteristic frequencies and gyroradii					
f_{pe}(kHz), av. (range) electron plasma freq.	450 (310–550)	130 (38–140)	20 (9–28)	3.5 (0.9–7.5)	
f_{pi}(Hz), av. (range) plasma freq. mass m_i ion	2500 (1900–5700)	850 (260–4300)	140 (150–4200)	25 (15–7300)	
f_{ce}(kHz), Eq. (lobe) electron cyclotron freq.	48 (58)	10 (13)	1.8 (3.2)	0.11 (1.2)	
f_{ci}(Hz), Eq. (lobe) cyclotron freq. mass m_i ion	1.5 (2.0)	0.5 (0.6)	0.09 (0.9)	0.01 (0.3)	
$\rho_{g,th}$ thermal ions gyroradii (km) Eq. (lobe)	1.8 (1.6)	8 (12)	36 (13)	530 (34)	
$\rho_{g,pu}$ pickup ions gyroradii (km) Eq. (lobe)	3.0 (2.5)	19 (15)	200 (110)	4200 (400)	

10. The estimates of satellite surface field assuming a dynamo magnetic field generation mechanism were given by Neubauer (1978), but here we use values inferred from *Galileo* flybys including for Io (Kivelson, unpublished 2003), Europa (Schilling *et al.* 2004), Ganymede (Kivelson *et al.* 2002), Callisto ((Kivelson, unpublished 2003).

11. The values of the Hall and Pedersen conductances (Σ_P and Σ_H) are obtained as follows: for Io from the numerical model, of Saur *et al.* (1999); for Europa from the numerical model of Saur *et al.* (1998), for Ganymede estimated from values of B (Kivelson *et al.* 1998), n_n (Hall *et al.* 1998), n_e (Kliore *et al.* 2001) for Callisto, estimated from values of B (Table 21.2), n_n (Carlson 1999) , n_e from Kliore *et al.* (2001). Averaged values for Io and Europa are also from the numerical model and are those required to match the overall calculated reduction factor for flow velocities. For Ganymede, the conductances Σ_P and Σ_H were integrated along the field lines in the open field line region. Values are small because Ganymede's internal magnetic field is large. Considerable uncertainties of the parameters n_e and n_n for Ganymede and Callisto imply large uncertainties of these conductances. For example, Eviatar *et al.* (2001b) give $\Sigma_P = 100$ S for Ganymede. Their number is calculated from estimated pickup rates also contributing to Σ_P. Values of Pedersen conductance given for Io from Cheng and Paranicas (1998), and from Paranicas *et al.* (1998) for Europa and from Eviatar *et al.* (1998) for Ganymede are much smaller than the values that we give here.

12. The estimate of $\dot{M}$ refers to additions in the region close to the satellite. For Io the value is based on spectroscopic observations of mass loading in the torus (Brown 1994, Thomas *et al.* 2001) and the first *Galileo* flyby of Io (Bagenal *et al.* 1997). Estimates of $\dot{M}$ for Europa, Ganymede, and Callisto caused by sputtering of H_2O molecules by high energy particles are from Ip *et al.* (1998) for Europa, from Paranicas *et al.* (1999) for Ganymede (with half from the polar caps and half from the closed field line region), and from Cooper *et al.* (2001) for Callisto.

Notes for Table 21.1

The first value of a parameter is the average inferred value in the vicinity of the near-equatorial current sheet. The second value in parentheses is the extremum value away from the equator. Where the variations are not systematically related to latitude, the range shows the minimum or maximum values measured or inferred. The velocity entries represent flow speed away from the immediate environment of the satellites.

For sputtering sources: the first estimate is obtained if all the sputtering ions are assumed to be protons. The bracketed estimates assume oxygen ions.

The sound speed c_s is $(\gamma p/m_i n_i)^{1/2}$ in terms of γ, the ratio of specific heat at constant pressure to the specific heat at constant volume, p, the total thermal pressure (including both ions and electrons) and m_i the average ion mass.

The Alfvén speed, v_A is $B/(\mu_o \rho)^{1/2}$ with B the field magnitude and $\rho \sim n_i m_i$ the mass density.

speeds but cannot propagate across the magnetic field. Electrical currents are present in all three wave modes, but only the intermediate wave, referred to as the Alfvén wave, carries current along the magnetic field. Energy and momentum can be transported in the magnetic field direction by Alfvén waves but only fast waves and, to a small extent slow waves, carry energy and momentum across the magnetic field.

The interactions between the Galilean satellites and the plasma of the jovian magnetosphere lead to changes in the local plasma through additions of new ions or through interactions that change the momentum of the plasma and produce heating or cooling. The interactions also can change the velocity space distribution of energetic particles, $f(\mathrm{v})$, where $\mathrm{v} = (\mathrm{v}_\perp, \mathrm{v}_{||})$ is velocity perpendicular and parallel to the magnetic field, and can generate strong electrical currents. Such effects localized near the moons produce beams, anisotropies, and other forms of free energy. Plasma wave spectra give evidence of the associated kinetic effects. The plasma waves observed include ion cyclotron waves driven by free energy associated with the ion pickup process, whistler mode emissions and electron cyclotron harmonic emissions presumably driven by positive values of $\partial f(\mathrm{v})/\partial \mathrm{v}_\perp$ in the suprathermal electron distributions, and electrostatic solitary structures or perhaps kinetic Alfvén waves. Not all of

Table 21.2. Dimensionless parameters characterizing plasma–satellite interactions.

Parameter	Io	Europa	Ganymede	Callisto	Titan
$M_A = u/v_A$ equator (range)	0.31 (0.16–0.39)	0.47 (0.08–0.59)	0.73 (0.05–1.1)	2.8 (0.02–8.5)	1.9
$M_s = u/c_s$ (range)	2.0 (1.0–2.1)	0.9 (0.16–1.1)	0.5 (0.06–0.8)	0.4 (0.03–1.2)	0.57
$M_f = u/(v_A^2 + c_s^2)^{1/2}$ (range)	0.31 (0.16–0.38)	0.42 (0.07–0.52)	0.42 (0.04–0.66)	0.39 (0.02–1.2)	0.55
v_ϕ/v_{cr}	1.0	0.8	0.8	0.6	
θ_A (degrees) (range)	17 (9–21)	25 (4.5–30)	36 (3–48)	70 (1–83)	62
$\beta = p/(B^2/2\mu_o)$ (lobe)	~0.32	~0.32	2.4 (0.8)	64 (0.6)	11
Σ_P(av)g/Σ_A(eq)	~45	6	0.5	86	
$\dot{M}/\rho_i u r_s^2$ (range)	1–3	1–3	5–500	4–4000	<600
B_{int}^{surf}/B_{bg} (range)	<0.02	<0.15	13–23	<(1–10)	≤2.3
$\rho_{g,pu}/r_s$ (range)	0.0014–0.0016	0.010–0.012	0.01–0.08	0.16–1.73	

these phenomena are observed at each of the Galilean satellites because conditions differ from one to another moon. It should be noted that these phenomena are not likely to be as significant energetically as the magnetohydrodynamic (MHD) interactions, but the plasma waves thermalize the free energy in the particle distributions or otherwise act to transform the energy realized through the interactions.

21.3.1 Thermal Plasma

Although the orbits of the Galilean moons lie almost in Jupiter's spin equator, they are tilted relative to the plasma torus and its extension into the equatorial plasmasheet of the middle magnetosphere. The highest density plasma is found near the centrifugal equator, which is inclined by θ_{tilt} of order 7° relative to the jovigraphic spin equator (Hill *et al.* 1974). The density falls off north/south of (above/below) the centrifugal equator with an e-folding distance – scale height – of ~1 R_J for a ~50–100 eV plasma. The scale height is smaller for less energetic particles, and thus the "effective temperature" (or second moment of the velocity distribution) increases with distance from the magnetic equator. As the moons move in their orbits, they effectively move up and down relative to the centrifugal equator, and the density and temperature of the local plasma change markedly. It is helpful to think of a moon as threading in and out of the densest part of the plasmasheet every few hours. Inside of ~20 R_J, a moon's maximum distance from the approximately planar surface on which the plasma density is largest is $r \sin\theta_{tilt}$ (with r the radial distance from Jupiter); therefore the north–south excursions increase linearly with r. The magnetic pressure (proportional to the field magnitude squared) changes in antiphase to the plasma pressure, with local minima where field lines cross the centrifugal equator. Because of the importance of plasma properties for interpreting satellite interactions, we next summarize what is known quantitatively about the plasma density in the vicinity of the moons.

In the vicinity of Io, local electron densities ranging from ~1350 cm^{-3} to ~4000 cm^{-3} have been observed (Gurnett *et al.* 2001, Frank and Paterson 2001a,b). Some of the variation represents temporal changes in the torus, yet there is also a factor of ~2.2 variation resulting from Io's motion in the torus (discussed in Chapter 23). The azimuthally symmetric model of the torus based on plasma measurements made by *Voyager 1* predicts a variation between ~2700 cm^{-3} when Io is at the N–S center of the plasma torus (SIII ~112° and ~292°) and <1200 cm^{-3} when Io is farthest from the torus center (SIII ~20° and ~200°) (Bagenal 1994). One way to separate spatial from temporal variations is to take the ratio of observed plasma density in the *Galileo* epoch (1995–2002) to the values predicted from the model developed for the *Voyager 1* epoch (1979). Such comparisons for all *Galileo* passes through the torus suggest that at the time of *Voyager 1* the torus density was particularly low, because the ratio of observed to modeled electron density varies from 1.15 (I27) to 1.67 (C23) (based on Gurnett *et al.* (2001), and Bagenal (1994)), though Frank and Paterson (2000) report densities on I24 that are lower than Voyager models.

The electron density at Europa's orbital distance is considerably smaller than that in the central torus. Based on the *Voyager 1* plasma conditions at the orbit of Io, the density model predicts values of 35–40 cm^{-3} off the equator and values of 80–110 cm^{-3} near the equator, depending on the strength of the equatorial current (which stretches the plasma-laden flux tubes of the torus radially outwards) (Bagenal 1994). Observed electron densities over several *Galileo* flybys of Europa spanning 3 years ranged from 18 to 250 cm^{-3} (Gurnett *et al.* 1998, Kurth *et al.* 2001). Europa sees a sinusoidal variation in the ambient density (due to the exponential variation in density with latitude) in addition to a factor of ~2 variability.

At greater distances from Jupiter, near the orbits of Ganymede and Callisto, the plasma is not only more tenuous but its density is increasingly variable. As the ~3 R_J thick plasmasheet flaps over Ganymede and Callisto, the ambient density changes by factors of ~5 and ~10 respectively. Callisto orbits far enough from Jupiter to experience the rapid temporal variability of the dynamic middle magnetosphere (discussed in Chapters 24 and 25).

21.3.2 Energetic Particles

Above about 10 keV, it is common to speak of "energetic charged particles," to distinguish this population from the lower energy plasma. The number density of the energetic particles in the magnetosphere is much smaller than the plasma number density, and the flux of the energetic particles falls off with increasing energy. For instance, the number of protons between 50–200 keV near Europa is about one-thousandth the total plasma density at a similar location

(Paterson *et al.* 1999, Paranicas *et al.* 2002). However, the energy density of the energetic particles is significant both to the structure of the magnetosphere and to the specifics of the interactions with the moons. It is also useful to keep in mind that energetic particle trajectories can significantly deviate from those associated with particles in the cold plasma.

Jupiter's magnetosphere, like Earth's, has regions in which the flux of quasi-trapped energetic particles becomes particularly large when compared with typical magnetospheric values or with the levels found in the solar wind near 5 AU. To appreciate this fact, consider that the intensities of tens to hundreds of MeV ions are much larger near the icy satellites than are the intensities of anomalous and galactic cosmic rays in the solar wind (Cummings and Stone 1998, Paranicas *et al.* 2001). Mauk *et al.* (1996) have shown that particles with energies from tens of keV to tens of MeV dominate some moments of the particle distribution. In Table 21.1, we reproduce their range of values for the pressure. Using *Voyager* data, Mauk *et al.* showed that energetic particles dominate the particle pressure at radial distances that include the orbits of some of the Galilean satellites. Mauk's work shows that the energy deposited on to the icy satellites by magnetospheric particles is carried principally by the energetic particles, not the plasma. We will discuss this further below, when we address satellite sputtering.

Mauk *et al.* (1998) pointed out that some moments of the distribution decreased between the *Voyager* and *Galileo* periods, whereas the thermal plasma density increased (see Chapter 23). An increase of neutral density can account for both observations. Mauk *et al.* (1998) have suggested that iogenic neutral gas whose density is greatest between the orbits of Io and Europa, serves both as a source of thermal ions and a sink for energetic particles through charge exchange.

21.3.3 Dimensionless Parameters Characterizing the Plasma-Moon Interactions

The plasma interaction with a planetary obstacle can be described generically for plasmas whose properties fall into classes defined by dimensionless parameters that conveniently indicate which of various physical processes are dominant. Table 21.2 provides some of the important dimensionless quantities of the plasma present near the orbits of the different moons. The Mach number or ratio of the plasma flow speed to the wave speed indicates whether information can or cannot propagate into the upstream fluid. For the conditions near the moons, the fast wave Mach number differs little from the Alfvén Mach number, M_A. At the locations of the inner three moons, the flow is never super-Alfvénic. It is likely that the flow becomes super-Alfvénic when Callisto is close to the center of the plasmasheet, and in this case, the interaction region would include a shock to slow the plasma, but *Galileo*'s close passes by Callisto have occurred far from the locations where such conditions occur and shocks have not been encountered. The periodic appearance and disappearance of a shock may produce detectable particle signatures near Callisto's orbit, but the point has not yet been addressed either through data or theoretically.

The quantity β in the table indicates where thermal plasma effects dominate field effects in much the same way as the Mach number identifies whether the flow speed or the wave speeds are dominant. When plasma effects dominate, a situation that may apply near the center of the plasmasheet in the middle magnetosphere, diamagnetic currents are important. Because $\beta^{1/2} = [2\mu_o p/B^2)]^{1/2} = (2/\gamma)^{1/2}(c_s/v_A)$, the sound speed exceeds the Alfvén speed when $\beta > (3)^{1/2}$.

In order to exert the forces that divert and slow the plasma flowing towards a moon, thermal pressure gradients and currents must link the moon (or its ionosphere or magnetosphere) to the plasma in its vicinity. It follows that the conductivity of the satellite and its ionosphere, represented by the height-integrated conductivity Σ_s, becomes important for controlling how much the plasma flow changes near the satellite. This conductivity must be compared with $\Sigma_A = (\mu_o v_A)^{-1}$, the conductance of the Alfvén waves (Goertz and Deift 1973) that carry the currents off into the plasma. Neubauer (1980) and Southwood *et al.* (1980) have discussed this point. They show that the degree to which the flow is slowed near the satellite is controlled by the ratio Σ_s/Σ_A. Σ_A varies with the mass density of the plasma. When this ratio is $\ll 1$, plasma flows directly to the surface. Conversely, for sufficiently small Σ_A, the plasma flowing towards the moon can be virtually halted by its presence and the flow diverges away from the conductor. The Alfvén conductance is quite well constrained by data, but conductivities and even the conducting paths at the satellites are much more uncertain, since there are contributions from the very inhomogeneous ionosphere and pickup. In particular, day/night asymmetry of a satellite's ionospheric conductivity maps along perturbed magnetic field lines and imposes corresponding asymmetry on the interaction region as has been pointed out for the interaction with Saturn's moon Titan (Ness *et al.* 1981, 1982, Hartle *et al.* 1982) and more recently for Jupiter's moons. Further complications arise because of direct coupling with Jupiter's ionosphere as discussed in detail in Chapter 22 and below.

The effectiveness with which mass loading and elastic and non-ionizing inelastic collisions extract momentum from the plasma flow affects the interaction. Each newly ionized neutral of mass m_i must be accelerated to the flow velocity $\mathbf{u}$ as it becomes part of the flowing plasma. (Here $\mathbf{u}$ is the velocity of the plasma relative to the moon on which it is incident.) The required acceleration is achieved by extracting momentum $m_i\mathbf{u}$ from the bulk plasma. With $\dot{m}_i$ as the rate of mass addition, the effectiveness of mass loading in slowing the flow over the cross section of the moon is determined by the value of $\dot{m}_i/\rho_i u r_s^2$ where ρ_i is the density of the background plasma. If the plasma density is low and the pickup rate great, the pickup ions can stop the flow, whereas high-density plasma may be little modified by pickup ions.

The dimensionless ratio B_{int}^{surf}/B_{bg} is also of importance in establishing the form of the interaction. It provides a rough estimate of whether a magnetosphere can form around one of the moons because it indicates whether magnetic pressure of internally generated fields exceeds the magnetic pressure of the external field. When the ratio is >1, a magnetic cavity surrounding the moon is likely to be able to form in the magnetospheric plasma; the magnetic field at Ganymede satisfies the inequality and does create a mini-magnetosphere, as discussed below.

21.4 BRIEF OVERVIEW OF THE THEORY OF SATELLITE INTERACTIONS

Models of Galilean satellite interactions date to the work of work of Piddington (1968) and Goldreich and Lynden-Bell (1969) who invoked the effect of plasma in motion relative to a conducting Io to explain how Io could control the emission of decametric radiation by Jupiter (Bigg 1964). They proposed that field-aligned currents couple Io to Jupiter's ionosphere through the magnetospheric plasma, but they supposed Io's conductivity to be so high that the jovian field was frozen in to Io. Their description of the interaction is referred to as the unipolar inductor model. Subsequent work casts a somewhat different light on the nature of the interaction with Io. Chapter 22 discusses the complexity of the Io interaction. Here we introduce some of the principal ideas that apply not only to Io's interaction but also to the interactions of the jovian plasma with other moons.

21.4.1 The Topology of the Interaction Region: The Alfvén Wing

The jovian magnetospheric plasma is coupled to Jupiter's ionosphere through the action of currents flowing along the planetary magnetic field (Hill *et al.* 1983). The coupling sets the plasma into motion so that it is approximately corotating with Jupiter, with a lag that increases in the middle and outer magnetosphere. The azimuthal velocity, v_ϕ, exceeds the orbital velocity, v_s, of each of the moons. Correspondingly, in the plasma rest frame, the moons move in the sense opposite to the direction of their orbital motion. The moons are large compared with the scale lengths that characterize the thermal plasma, such as the heavy ion gyroradii (see Table 21.2).

In the rest frame of the moon, the interaction is approximately static and standing MHD waves bound the region of interaction. A schematic of the interaction is shown in Figure 21.1. $\mathbf{B}_o$ represents the unperturbed ambient magnetic field and the plasma flows from left (upstream) to right (downstream). Here $u = v_\phi - v_s$ represents the plasma flow velocity in the satellite's rest frame. As noted previously, the wake extends ahead of the satellite in the direction of its orbital motion. Compressional perturbations that slow the upstream plasma propagate effectively across the field and produce small amplitude non-localized disturbances found upstream of the moon in the figure. However, the field rotations that divert the flow around the body must be imposed by shear Alfvén waves, the MHD mode that carries field-aligned currents. These waves produce changes that propagate along $\pm\mathbf{B}_o$ at the Alfvén velocity in the plasma rest frame. When viewed in the satellite rest frame, the perturbations associated with the field aligned currents appear within wedge-shaped regions referred to as the Alfvén wings whose upstream boundaries are shown as heavy black lines at an angle $\theta_A = \tan^{-1}(u/v_A)$. The divergence of the flow occurs not only in the regions near the conducting moon, but also around the Alfvén wings that extend both above and below as illustrated schematically in Figure 21.2.

The Alfvén wing structure was first discussed by Drell *et al.* (1965) in the context of low-altitude Earth orbiting vehicles. Later work by Goertz and Deift (1973), Goertz (1980), Neubauer (1980, 1998b,a, 1999a,b), Southwood and collaborators (Southwood *et al.* 1980, Southwood and Dunlop 1984, Wright and Southwood 1987, Southwood and Fazakerley 1992) and Linker and collaborators (Linker *et al.* 1991, 1998, 1999) have added considerably to the first description of the properties of the interacting system. In particular, the role of the slow mode waves in restoring pressure equilibrium in the downstream regions has been recognized (Linker *et al.* 1991, Neubauer 1998b). The conclusion that strong perturbations of the field and plasma properties are found downstream of a tilted boundary and decrease in magnitude with distance upstream of it has been amply confirmed. Within the geometric flux tube (*flux tube* in the figure) but outside the Alfvén wing, the perturbations are weak.

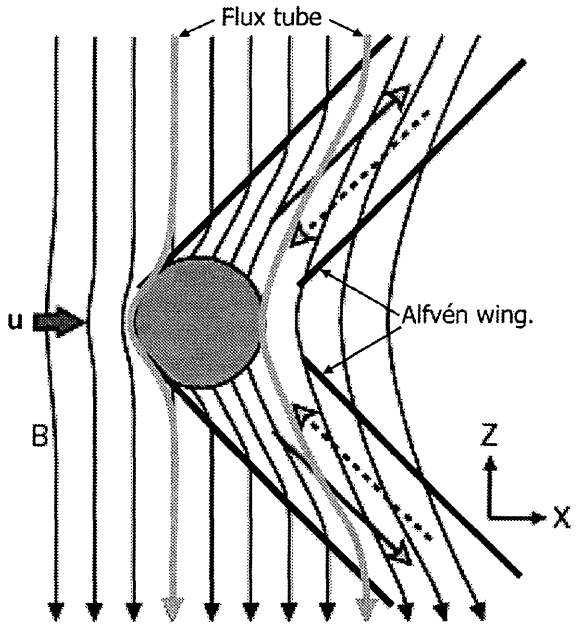

Figure 21.1. Schematic representation of the Alfvén wing disturbances arising in a plasma with $M_A < 1$. The background field of Jupiter (**B**) is southward. The sketch represents a cross section viewed from larger radial distance looking inward towards Jupiter, with flow (**u**) from left to right. Current paths (open arrowheads) are represented with solid lines for current flowing on the side radially away from Jupiter and with dashed lines for current flowing on the side closer to Jupiter. Some field compression and bending occurs upstream of the region of the major interaction. The front across which the field bends significantly out of the plane is indicated with a heavy black line and bounds the Alfvén wing. The Alfvénic perturbation does not affect the field magnitude, so although the spacing of field lines entering the conductor increases within the Alfvén wing in the sketch, some of these field lines do not lie in the plane of the image. The flux tube, bounded by the gray lines, is defined as field lines that enter Io and differs from the Alfvén wing.

21.4.2 Interaction with the Thermal Plasma and Field and with Jupiter's Ionosphere

The description of Alfvén waves propagating away from Io differs in some ways from the unipolar inductor model of Goldreich and Lynden-Bell (1969) but the geometry of the local current system differs little. Hill *et al.* (1983) point out

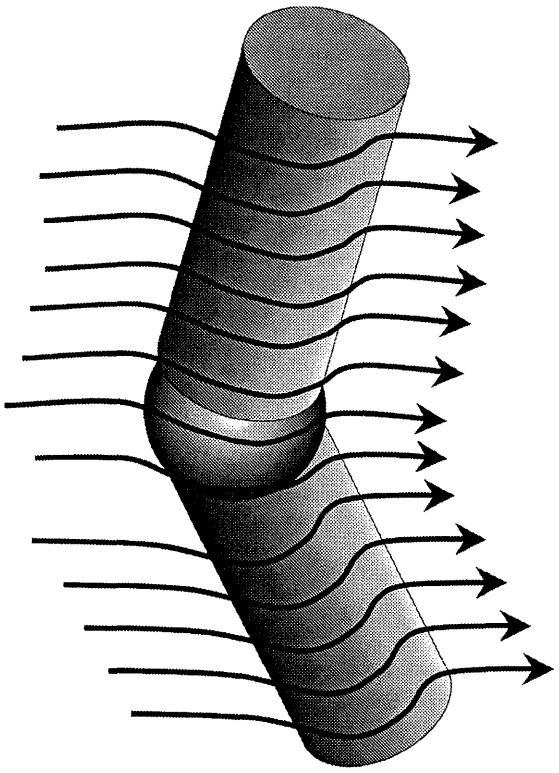

Figure 21.2. Schematic illustration of the diversion of plasma flow around a conducting moon and the Alfvén wings that are linked to it.

that the unipolar inductor model represents the limiting case in which Σ_A becomes so small or v_A becomes so large that the round trip wave transit time to the jovian ionosphere τ_J is small compared with the time τ_s for plasma to flow across the satellite. In this limit the reflected wave returns to the equator within one satellite diameter, and the current through the moon is controlled partially by the conductivity of Jupiter's ionosphere. Multiple wave reflections strongly modify the interaction region.

The reference to the jovian ionosphere, the first mention in this chapter of boundary conditions along field lines, suggests that non-local aspects of the interaction problem may be important; indeed this is likely to be true for Io. Barbosa (1981), referring to *Voyager 1* measurements, concluded that $\tau_J/\tau_s > 1$ except possibly when the satellite is at an extremum of magnetic latitude near the edge of the plasma torus. The evidence of strongly slowed flows and extremely high plasma density from *Galileo*'s passes by Io led Crary and Bagenal (1997) to consider how the significant slowing of the flow across the polar cap would affect the interaction. Although the time to flow over Io at the unperturbed flow speed may be small compared with the transit time to Jupiter ($\tau_J/\tau_s > 1$), implying that a local interaction is all that need be considered, the large ion pickup rate at Io plus the contribution from the ionospheric interaction appears to slow the flow enough that the inequality reverses sense ($\tau_J/\tau_s \ll 1$), producing a compound structure, part Alfvén wing and part unipolar conductor. For the moons other than Io, the transit time to Jupiter is long compared with the flow time, and the Alfvén wing description based on local plasma conditions seems the relevant interpretation.

Although the jovian ionosphere probably does not influence the interaction region except at Io, the Alfvén waves launched from the moons do affect the jovian ionosphere. Decametric emissions from Jupiter's ionosphere are thought to be triggered by Alfvén waves launched from Io (see review by Carr *et al.* 1983) and to be the source of Io-related radio bursts at frequencies of tens of MHz observed at Earth as discussed in Chapter 24. Multiple reflections of the Alfvén waves may account for the arc structure observed by *Voyager* instruments (Gurnett and Goertz 1981, Bagenal and Leblanc 1988, Leblanc *et al.* 1994). Ganymede and Callisto impose a weak control on the intensity of hectometric and decametric (3.2–5.6 MHz) jovian radio emissions. As in the case of the familiar Io control of decametric emissions (see Chapter 22), these emissions are most probable when the controlling satellites are at specific phases in their orbits as viewed by the observer (Menietti *et al.* 1998, 2001). Most dramatically, bright spots of infrared (Connerney *et al.* 1993) and ultraviolet (Clarke *et al.* 1996) emissions appear at the magnetic footprints of Io, in the jovian ionosphere. Ultraviolet emissions are also found at the footprints of Europa, and Ganymede (Clarke *et al.* 1998) and, for Io, a narrow bright feature extends ahead of the footprint (in the sense of orbital motion) along the ionospheric boundary of the Io magnetic shell. It can be said that the signature of the plasma–moon interactions is beamed to great distances in the solar system through coupling with the jovian ionosphere.

21.4.3 Modifications Resulting from Mass Pickup

When neutrals are ionized and new ions are added to the flowing plasma, currents are generated. This is because a neutral (on average at rest in Io's frame) experiences an electric field $\mathbf{E} = -\mathbf{u} \times \mathbf{B}$ in the presence of the flowing plasma. When the neutral is ionized, the electric field accelerates the ion in one direction (radially outward for the conditions near the moons of Jupiter) and the electron in the opposite direction. As illustrated in Figure 23.6, the resulting trajectories drift in the direction of plasma flow with mean velocity $\mathbf{u}$, while magnetic forces impose gyration with speeds perpendicular to the background magnetic field equal to the background flow speed. The currents arise because the gyrocenters of the two charge species separate by the sum of their gyroradii (roughly $r_{L,i}$) implying that the current density is $j = e\dot{n}_n r_{L,i}$ if the ionization rate per unit volume is $\dot{n}_n$. This current flows across the field, but the requirement that current be divergenceless requires an associated development of field-aligned currents. It has been shown by Neubauer (1998b) and Hill and Pontius (1998) that with regard to the current or conductivity distribution, the effect of mass loading can simply be taken into account by addition of an appropriate contribution to the collision frequencies.

Goertz (1980) pointed out that pickup currents may be dominant in the immediate vicinity of Io. Southwood and Dunlop (1984) pointed out that an upstream–downstream asymmetry develops when new ions slow the plasma as they are picked up near the satellite. Ultimately all the plasma must re-accelerate to the incoming flow speed, but even if all the momentum extracted from the upstream flow is returned

to the plasma in the downstream region, it will be insufficient to restore corotation to the portion of the downstream flux tube on which the density has increased. Inertial currents (equal to $\rho_d B \times (u \cdot \nabla)u/B^2$ in terms of the local plasma velocity, **u**, and the downstream density, ρ_d) act to restore corotation over a wake distance $L_W = 2\ell/\alpha^2$, where ℓ is the distance along the flow direction over which mass is added, and α is the fractional reduction of velocity near the moon. If the velocity drops close to zero, the length of the wake can be orders of magnitude greater than the length over which ions are picked up. Over this entire distance, field-aligned currents will act to feed the perpendicular currents that restore corotation, and this may account for the long trail that leads Io's footprint in the jovian ionosphere (Hill and Vasyliunas 2003, Delamere *et al.* 2003, Su *et al.* 2003).

Mass pickup, although present at all of the moons, is critical at Io's orbit where maintenance of the plasma torus requires of order 10^{28} ion s^{-1} (Richardson and Siscoe 1981, Brown 1994), though there is debate over the fraction of the new material ionized near Io (Smyth 1998, Bagenal *et al.* 1997, Saur *et al.* 2002).

Near Europa, there is evidence for a source of icy material (Intriligator and Miller 1982, Bagenal *et al.* 1992, Paterson *et al.* 1999, Volwerk *et al.* 2001) that suggests that a near-Europa mass-pickup wake may exist. The signs of a Europa source are partially masked by the large ion background of the torus making the additional contributions difficult to discern, but the possibility of a Europa plasma torus was discussed in detail by Schreier *et al.* (1993) who inferred an upper limit of 15% for the contribution of Europa to the plasma near its orbit.

An interesting feature of a pickup ion distribution is that it is strongly anisotropic with the ions distributed in a ring with perpendicular velocity magnitudes close to u and much smaller field-aligned velocities. The implications of the anisotropy are discussed in Section 21.5 in relation to observations.

21.4.4 Interaction with Magnetized Bodies

An important hint of interior structure of a planetary body is given by its internal magnetic field. A permanent magnetic moment (i.e., one that persists over millennia) requires a heat source to drive convection. For Io, it was known that tidal stress provides a mechanism for heating the shallow interior (Peale *et al.* 1979); active volcanoes confirmed the presence of subsurface melt (Morabito *et al.* 1979) and its global distribution was revealed by the planet-wide distribution of plumes and hot spots (Lopes-Gautier *et al.* 2000). A near surface heat source, however, does not necessarily drive a dynamo. The convection that generates the dynamo currents arises most naturally from heating at depth, with subsequent flow arising from the increased buoyancy of the heated material. Nonetheless, computer models in which tidal heating generates internal fields have been developed by allowing for time-dependent imbalances between sources and losses of heat (Wienbruch and Spohn 1995), or by imposing a seed field in an MHD simulation (Glatzmaier *et al.* 1998) and taking into account departures from spherical symmetry of the heat sources (Tackley *et al.* 2001).

In Section 21.5.2, we noted that time-varying external fields can drive an inductive magnetic field in a moon. The component of the magnetospheric magnetic field aligned with a moon's spin axis changes little over a synodic period, but the components perpendicular to the spin axis (approximately uniform spatially across the diameter of a moon) vary in time so the induced dipole moment lies in the equatorial plane and reverses its direction periodically. An induced dipole field requires that there be a global electrically conducting shell in the interior. The outer shells of the three outer Galilean moons are formed largely of water ice and other low-density materials. In the solid state, ices have low electrical conductivity, except possibly for ice that is highly contaminated or very near its melting temperature. The detection of an induced field strongly suggests that a layer of melt, i.e., a layer of liquid water, is present within the icy shell but below the surface (Spohn and Schubert 2003).

The induced field imposes its imprint on the interaction with the surrounding plasma (Neubauer 1999a). At the surface of the conducting, current-carrying shell, the component of the total magnetic field radially out from the center of the body must vanish. This condition implies that the induced magnetic field creates a north–south asymmetry, which leads to skewed boundaries of the Alfvén wings, as illustrated in A and C of Figure 21.3.

The presence of a permanent internal magnetic moment greatly modifies the interaction between the moon and its surroundings if the magnetic pressure ($B^2/2\mu_o$) above the surface of the moon exceeds the total pressure exerted by the ambient magnetospheric plasma. The total pressure in the plasma includes thermal pressure, magnetic pressure, and flow dynamic pressure ($\sim\rho u^2$), where ρ is the plasma density. By recognizing that the ratio of the thermal and flow pressure to the magnetic pressure are approximately β and M_A^2, respectively, and that these quantities are <1 except possibly when Ganymede and Callisto are near the center of the plasmasheet (see Table 21.2), one finds that the total plasma pressure is typically well approximated by the magnetic pressure alone in the vicinity of the Galilean moons.

Estimates of the magnitude of a dynamo-driven internal magnetic moment based on the rotation rate and size of the Galilean moons (Neubauer 1978) suggested that the interaction with the surrounding plasma might be significantly modified by internal fields (Kivelson *et al.* 1979), but prior to 1995, only the quite distant *Voyager 1* pass by Io (Neubauer 1980) had occurred and that pass did not place meaningful constraints on internal field properties of these bodies. However, Table 21.2 shows that, at least for some of the moons, the internal fields dominate the external fields in their vicinity. If the magnitude of the moon's equatorial surface field exceeds that of the external field, most of the plasma is diverted around a roughly bi-cylindrical region (i.e., the regions above and below the mid plane bounded by dashed lines in Figure 21.4), the magnetosphere within which the moon is embedded. Details of the field topology depend on the orientation of the internal dipole moment, and here we assume that the magnetic moment is oriented antiparallel to the moon's spin axis, a situation that roughly describes Ganymede (Kivelson *et al.* 1997a). In such a case, the internal and external fields are nearly antiparallel and can reconnect near the moon's equator to produce a magnetic configuration that is reasonably well approximated by the schematic Figure 21.4. The cross section radius at the equator is

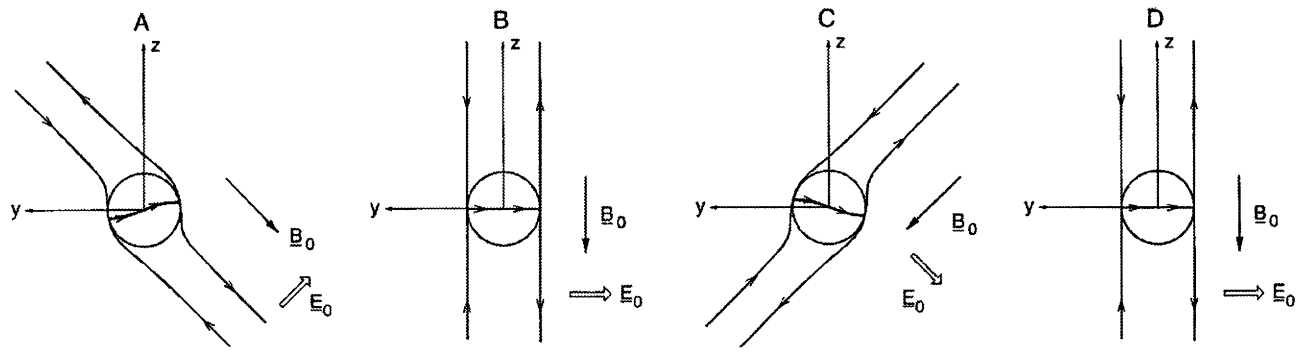

Figure 21.3. Schematic of the Alfvén wing structure expected near Callisto viewed from upstream looking in the direction of the plasma flow (from Neubauer 1999). The system is shown at 4 different times within one synodic rotation period. In panel A (C), Callisto is farthest above (below) the magnetic equator and in panels B and D, it is at the equator. Arrows represent current flow directions. The background electric (E_o) and magnetic (B_o) field directions are indicated. The changing Alfvén wing structure arises because of the induced magnetic moment which is absent in B and D, and is finite with orientation along the y axis in A and the $-y$ axis in C.

(approximately) established by the requirement that the magnetic pressures balance on the two sides of the boundary, i.e., $r_{\rm boundary}/r_{\rm p} = (B_{\rm dipole}/B_{\rm ext})^{1/3}$ where $B_{\rm dipole}$ is the equatorial surface field magnitude. For Ganymede, the field ratio is 7.5, implying that the boundary stands $\sim$2 R_G from the center of the moon.

Figure 21.4 represents the form of the field and the flow in a plane containing the unperturbed plasma velocity and the spin axis, as if seen from a location farther from Jupiter looking inward. Field lines of three different types are illustrated; some have both ends on the moon (closed field lines), some have only one end on the moon with the other end reaching Jupiter's ionosphere (open field lines), and some have neither end on the moon (jovian field lines). Heavy dotted lines represent the surfaces that bound the different types of field lines. The outermost dotted lines lie on the surface that defines the obstacle to the plasma. Above and below the moon, the bundles of field lines bend in the direction of the flow, indicating that even for a magnetized moon, Alfvénic perturbations affect the geometry of the interaction region. Within the magnetosphere, flow takes newly reconnected plasma over/under the poles and carries it to a downstream reconnection line from which flow at low latitude returns it to the upstream boundary.

The magnetospheric form with little upstream–downstream asymmetry, but with extended lobes transverse to the incident plasma flow direction, differs dramatically from the bullet-like form of a planetary magnetosphere. The critical difference arises from the fact that for a Galilean moon, the external magnetic pressure that confines the magnetosphere acts perpendicular to the spin axis, about which it is approximately axially symmetric, whereas a planetary magnetosphere is confined by the super-Alfvénic flow dynamic pressure on its upstream side but not on its downstream side. Our discussion of the Alfvén wing is not applicable to the interaction of a magnetized planet with the super-Alfvénic solar wind because it ignores the role of the bow shock. On the other hand, for a planetary magnetosphere the fact that the incident flow velocity greatly exceeds the group velocities of MHD waves dictates the form of the asymptotic bow shock and of the magnetotail boundaries and accounts for the bullet-like shapes of the magnetospheric cavities.

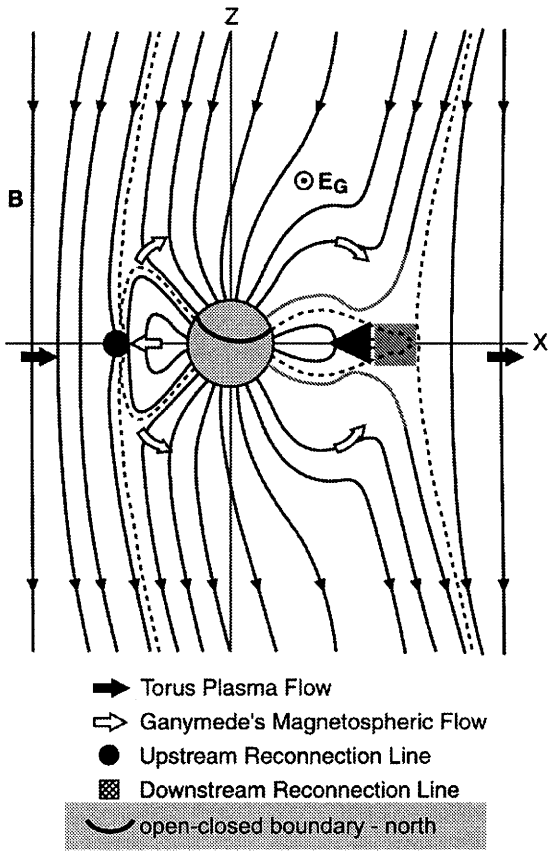

Figure 21.4. The form of the field and the flow in the vicinity of a magnetized moon like Ganymede. The schematic is in a plane containing the unperturbed plasma velocity and the spin axis, viewed from outside the moon's orbit looking radially inward towards Jupiter. Heavy dashed lines represent surfaces separating field lines of different types as discussed A thick curve in the ionosphere that trends towards lower latitude along the direction of flow indicates the location of the boundary between open and closed field lines in the northern hemisphere. Return flow is in the direction of the arrowhead next to the downstream reconnection location.

21.4.5 Special Considerations for Energetic Particles

Energetic particles trapped in the jovian magnetic field bounce rapidly along field lines between mirror points as they drift azimuthally. Except for the very highest energy particles, magnetic drift velocities are small compared with corotation drift velocities. However, in the interaction with a moon, the ratio of the bounce time, τ_b, to the time to flow across the satellite, τ_s, determines the types of responses observed in particle fluxes. Particles of energy high enough that $\tau_b/\tau_s \ll 1$ are removed from the plasma by collisions with the atmosphere or surface of a moon, producing gaps in the distribution functions observed along the flux tube and downstream of the body. For the jovian satellites, losses of energetic particles are most prominent in the downstream plasma. However, on the upstream side, losses have been observed at specific viewing orientations of particle detectors. For instance, for sufficiently high energies, ion gyroradii can become comparable with the radii of the moons, and then significant spatial asymmetries develop in the phase space distributions. A particle detector will register voids when oriented to detect ions whose trajectories pass through the moon at some phase of their gyromotion. Asymmetries of distributions arise because ions drifting with gyrocenters slightly displaced radially inward of a moon may be preferentially lost compared with those whose gyrocenters are displaced outward by the same distance. In another vein, very energetic electrons whose magnetic drift speeds are opposite to the corotation direction and larger than the plasma flow speed should have a wake upstream of the moon. In the downstream region, the localized decreases are referred to as microsignatures of the moons. The decreases can be strong functions of both spatial position and particle pitch angle (Mead and Hess 1973). Ions with drift orbits on the magnetic flux shell of a moon and with equatorial pitch angles near 90° can escape absorption if they drift past the moon's flux tube when the moon is located well off the equator, whereas ions with small equatorial pitch angles and short bounce periods will collide with the moon as they drift by.

The loss of energetic particles through interaction with a moon is observed as a dip in the particle flux centered at the moon's magnetic shell, even well away from the instantaneous position of the moon. Losses are balanced by radial diffusion, so the character of the flux depressions have proved to be of considerable value for studies of radial diffusion rates (for example, Thomsen *et al.* (1977), Schardt and Goertz (1983)). Empirical evidence suggests that energetic charged particles are lost heavily to the jovian satellites (Paranicas *et al.* 2000). The pattern of losses is frequently detected with enough accuracy to understand properties of the satellite, such as the boundary of the region of closed field lines in Ganymede's magnetosphere (Williams *et al.* 1998). The ongoing investigation of electromagnetic fields close to the satellites will clarify just which energies and species are deflected and which collide with the surface or sputter the atmosphere.

21.4.6 Simulations of the Interactions

Theoretical considerations of the complex form of the interaction between a flowing plasma and the moons of Jupiter have established many important aspects of the controlling mechanisms, but analytic solutions cannot capture the full complexity of the interactions. Numerical simulations have proved valuable in providing more complete descriptions. Although constraints of space preclude extensive discussion, we provide references to some of the interesting work that has been done, and then comment on the challenges that face the simulators.

Simulations for Io have been published by Wolf-Gladrow *et al.* (1987), Linker *et al.* (1988, 1991, 1998), Combi *et al.* (1998), Saur *et al.* (1999, 2000) and Kabin *et al.* (2001) and are discussed in Chapter 22. For Europa, simulations have been developed by Saur *et al.* (1998), Kabin *et al.* (1999), and Liu *et al.* (2000). For Ganymede and Callisto, no published simulations are yet available. The results of the different approaches are qualitatively similar. However, there are quantitative differences among the results, as inevitably the relevant physics is not completely incorporated and each simulator selects different aspects of the problem to treat with particular attention.

Most simulations for the interactions with the Galilean moons have been carried out in the single fluid MHD limit. Quantitative solutions are sensitive to the spatial resolution of the elementary cells, the size of the simulation box, the conditions imposed on the external boundaries and the assumptions made on the nature of the interaction at the moon itself, including assumptions of how the ionospheric conductivity is handled or the way in which mass loading is treated. Mass loading may be handled in terms of a spherically symmetric neutral source or may allow for a non-symmetric contribution.

In the sub-Alfvénic regime relevant to the Galilean moons, the upstream boundary conditions present challenges not encountered in the simulations of planetary magnetospheres where inflow plasma conditions cannot be modified by disturbances propagating against the flow. Various devices are introduced to deal with this difficulty, which is largely overcome by increasing the size of the simulation box. None of the simulations has tackled the critical issue of how the disturbances propagate through the tenuous region between the torus and Jupiter, nor how they couple to Jupiter's ionosphere (see Chapter 22 for further discussion of these issues).

In an MHD simulation, the effects of ion pickup differ depending on the mechanism of ionization and the net pickup rate. When ionization arises from electron impact, the flux tube content of the local plasma increases and the flow slows while conserving momentum density. When ionization results from charge exchange, the flux tube content does not change, but the momentum density decreases because each charge exchange neutral carries off some of the flow momentum. The contributions of charge exchange and other atomic processes modifying the flow add to the inherent non-linearities of the MHD problem. If the flow starts to slow in a spatial region with a high neutral density, the contact time increases and additional charge exchange interactions or collisions with ionospheric neutrals on the slowed flux tube result in further slowing. If the slowed flux tubes remain in regions of high neutral density, the plasma density can build up to extremely high levels. The plasma temperature (again in a generalized sense of the second moment of the distribution function) is also sensitive to the flow speed

at the point of pickup. If the flow speed is greater than the plasma thermal speed, as for example on the flanks where the flow accelerates, pickup ions increase the thermal energy per particle in the plasma and, conversely, if the flow speed is smaller than the plasma thermal speed, pickup ions reduce the thermal energy per particle in the plasma. It then follows that assumptions regarding details of pickup may produce many of the differences among results reported by different simulators.

Details of the satellite ionosphere also modify the interaction and it remains unclear how strongly such aspects as day-night asymmetry, localization of sources of volatiles, and variations of atmospheric composition affect the interactions. Some of the simulations (e.g., Saur *et al.* 1998, 1999, 2000) abandon the MHD formulation and adopt a multifluid description, sacrificing self-consistency in the treatment of the magnetic field in order to focus on a more correct description of the ionospheric effects. Some of the simulations introduce special constraints that improve the agreement with observations. For example, Kabin *et al.* (2001) find that currents coupled directly (without lag) to the jovian ionosphere improve the agreement between simulated magnetic profiles and observations in the December 1995 pass by Io, but it is hard to understand the mechanism that produces this effect.

None of the simulations yet deal with subtleties such as finite gyroradius effects or other perturbations on scale sizes small in comparison with the radii of the moons that may be important in producing dramatic features in the data such as electron beams (Frank and Paterson 1999a, Williams *et al.* 1996) or mirror mode waves (Kivelson *et al.* 1996a,b). These and other features of plasma–satellite interactions will most likely be incorporated into future simulations, which can be tested not only against the *Galileo* in situ observations but also in the context of the increasingly detailed remote observations that can monitor the temporal variability of the system (e.g., Connerney *et al.* 1993, de Pater *et al.* 2001, Clarke *et al.* 1996, Feldman *et al.* 2000, Oliversen *et al.* 2001). The ultimate challenge of dealing self-consistently with iogenic and other neutral populations would require combining large neutral dynamics codes to the MHD simulations, but such ambitious undertakings are beyond current computational capabilities.

21.5 OBSERVATIONS OF INTERACTIONS AT GALILEAN SATELLITES

In this Section we shall discuss some salient aspects of our present understanding of the plasma interactions at each of the moons, using mostly data from the *Galileo* orbiter, especially the fields and particles investigations (Frank *et al.* 1992, Gurnett *et al.* 1992, Kivelson *et al.* 1992, Williams *et al.* 1992).

21.5.1 Io: Properties of a Dynamic Environment

The interaction of the magnetospheric plasma with Io is discussed extensively in Chapter 22. Here we introduce aspects related to the general subject of the plasma–moon interaction. Our insight into the process is based on measurements made on close passes, supplemented by inferences from imaging and radio science.

The first close pass occurred in 1979 when *Voyager 1* passed ~20 000 km below Io, somewhat upstream of the Alfvén wing. The next opportunity to observe the interaction occurred in 1995 when *Galileo* passed Io near its equator, downstream in the flow at ~900 km altitude. Signatures of the interaction were observed in the magnetic field (Acuna *et al.* 1981, Kivelson *et al.* 1996a,b), in plasma waves (Gurnett *et al.* 1996a) and in plasma and energetic particle properties (Belcher *et al.* 1981, Frank *et al.* 1996, Williams *et al.* 1996). The magnetic perturbations were qualitatively consistent with expectations based on the Alfvén wing/unipolar inductor model, but appeared to require a conducting volume larger than Io itself. This can occur if the cross-field currents are carried in an ionosphere that extends to 1.4 R_{Io} or flows also in a pickup cloud, or if Io has an internal magnetic field. The ambiguity is related to the fact that the first measurements were made on flyby orbits, one well below the location of the moon (the *Voyager 1* flyby at 20 000 km south of Io) and one downstream of the moon (the initial *Galileo* flyby in 1995). At these locations the perturbation current system can mimic or mask the effects of an internal field. For example, the Alfvén wing/unipolar inductor closure current depresses the magnetic field downstream of a moon, a depression that can also be modeled with an internal dipole moment oriented antiparallel to the spin axis. In *Galileo*'s initial pass downstream of Io, a large magnetic field depression was proposed to be the signature of an internal magnetic dipole moment (Kivelson *et al.* 1996a,b, Kivelson *et al.* 1996, Kivelson *et al.* 1997b, 2001a) although alternative interpretations based on strong currents in the Alfvén wing system were offered (e.g., Neubauer 1998a, Linker *et al.* 1998, Hill and Pontius 1998). Numerical simulations shed very valuable light on the way in which pickup and extended ionospheres can account for the measurements from *Galileo*'s first Io flyby (Linker *et al.* 1991, 1998, 1999, Combi *et al.* 1998, 2002, Saur *et al.* 1999). The interpretation of the measurements in terms of extended current systems rather than an internal field proved to be correct, but confirmation awaited data from multiple passes at different locations relative to the background field and the flow direction.

Additional passes occurred in 1999 at ~600 and 300 km altitude and in 2000 at ~2000 km altitude. Although the second pass of 1999, polar and at low altitude, was designed to remove the ambiguity of interpretation by having the trajectory pass over the northern polar regions, where signatures from the Alfvén wing and from an internal dipole moment would differ markedly, a spacecraft anomaly led to loss of data other than that of the plasma wave investigation (Gurnett *et al.* 2001) and left the nature of the interaction ambiguous (Kivelson *et al.* 2001a). The other two passes were upstream passes at relatively low latitudes. Evidence of field pile-up consistent with slowed flow upstream of Io and of flow diversion with acceleration around Io (Kivelson *et al.* 2001a, Frank and Paterson 2000) did not provide insight into the properties of a putative internal field. The two passes of 2001 were polar passes at low altitude that made it clear that an internal magnetic field is negligibly small and probably absent (Kivelson *et al.* 2001b, Khurana *et al.*

2002). Data from a final pass in 2002 were lost as result of another spacecraft anomaly.

The polar passes revealed large increases of the plasma density over the polar cap that have been interpreted as entry into the ionosphere (Gurnett *et al.* 2001, Frank and Paterson 2001a) or into a flux tube magnetically linked to Io itself (Kivelson *et al.* 2001a) on which the flow is greatly slowed and the pickup plasma is exceptionally dense (Kivelson *et al.* 2001a, Linker *et al.* 1999). Neubauer (2000) pointed to the difficulty of generating locally high plasma density in a region of low neutral gas densities above the poles suggested by HST observations (Strobel and Wolven 2001). It is possible that plasma flows along the field lines from lower latitudes via slow mode disturbances (see also Chapter 22).

The plasma density was also extremely high in the near equatorial wake (Frank *et al.* 1996, Gurnett *et al.* 1996b). Interpretations of the high-density regions as the ionosphere (Frank *et al.* 1996) or as the extension of the region of stagnated flow (Linker *et al.* 1998) have been offered. The latter interpretation recognizes that pickup densities can become large if flux tubes remain linked to the region of the densest neutral source for times long compared with the ~1 minute required for the unperturbed flow to cross an Io diameter as suggested for the hybrid Alfvén wing/unipolar inductor model of Crary and Bagenal (1997). In regions of slowed flow, pickup ions are not only dense, they are also cold, i.e., possibly little different from ionospheric plasma because their gyrovelocity is of order the flow speed. The ionosphere is likely to be rich in pickup ions, so the distinction may not be meaningful. Within the downstream region of dense plasma, strongly field-aligned beams of energetic electrons were observed (Frank and Paterson 1999a, Williams *et al.* 1996, Williams 2001), consistent with strong coupling to the jovian ionosphere, and possibly related to the auroral emissions observed at the foot of the Io flux tube (Connerney *et al.* 1993, Clarke *et al.* 1996) discussed more fully in Chapter 26.

The neutral cloud arising from the Io interaction has dramatic consequences for the entire jovian system. The heavy ion source not only modifies the structure of the jovian magnetosphere (Hill *et al.* 1974) and dominates its dynamics (Southwood and Kivelson 2001) but also produces radiation visible from Earth. We have commented on the radiating regions that include a neutral sodium cloud of order 1 R_J in length that moves with Io around its orbit (Smyth and McElroy 1977, Burger *et al.* 1999) and a fainter disk-like cloud that surrounds the entire jovian system out to a distance of hundreds of R_J (Mendillo *et al.* 1990, 1992). Although sodium is only a trace element in the sputter source, both of these features are observed in a spectral line of neutral sodium that scatters sunlight strongly. The distance to which the sodium atoms sputtered from Io disperse before they are ionized determines the shape and extent of the sodium cloud localized near Io. The more extended disk forms as a result of a two-step process in which ionized sodium atoms, corotating with Jupiter, undergo charge exchange with a neutral atom at rest relative to Io, thereby forming fast moving neutral atoms that escape to large distances before being ionized.

The dominant ions throughout the jovian magnetosphere are iogenic sulfur and oxygen. Emissions from sulfur (Mekler and Eviatar 1974, Brown *et al.* 1983, Schneider and Trauger 1995, Woodward *et al.* 1994) and oxygen (Scherb and Smyth 1993) have been monitored from the ground and have been used to characterize the torus of heavy ion plasma that surrounds Io's orbit (Bagenal 1994) and is the source of the current-carrying plasmasheet that extends outward and distends the middle magnetosphere of Jupiter (Smith *et al.* 1974, Acuna *et al.* 1983). Spectroscopic studies of the torus radiation in the ultraviolet by *Voyager* (Shemansky and Smith 1981, Taylor *et al.* 1995) and more direct measurement by the *Galileo* plasma instrument (Frank and Paterson 2001a,b) provided information on the charge states of ions in the torus (see Chapter 22).

The pickup ion population has also been characterized by studies of plasma waves in the vicinity of Io. Narrow-banded emissions near the plasma frequencies of the molecular ions SO^+ and SO_2^+ were observed near Io and identified as ion cyclotron waves (Kivelson *et al.* 1996a,b, Warnecke *et al.* 1997, Huddleston *et al.* 1997, Russell *et al.* 1999, Russell and Kivelson 2000). The generation of such waves can be understood by noting that pickup ions acquire momentum only in the direction transverse to the magnetic field, resulting in an anisotropic velocity distribution. Waves can grow if the anisotropy of the full distribution including both the pickup ions and the background plasma is sufficiently large. For species such as S^+ and O^+ that dominate the background plasma, the net anisotropy is too small to produce ion cyclotron waves, but molecular ions have short lifetimes under conditions relevant to the plasma torus, and are absent in the background plasma. Their distribution is consequently highly anisotropic near Io's position.

It is not yet fully understood why SO^+ was present on some passes and not on others (Russell *et al.* 1999, Russell and Kivelson 2000). Speculative interpretations suggest that the composition of the neutral source may depend on the location of closest approach to Io or on the location of closest approach relative to the illuminated hemisphere, or that changing composition may result from temporal variations of volcanic activity or from the local time of Io's position relative to Jupiter during the flyby.

At higher frequencies, relatively narrow-banded emissions in Io's wake have been attributed to Doppler-shifted ion cyclotron waves generated by a non-thermal distribution of protons (Chust *et al.* 1999). The presence of protons with ring distributions characteristic of newly picked-up ions in the vicinity of Io is also reported by Frank and Paterson (1999b).

In the region downstream of Io, the flow that slows as it passes Io must reaccelerate to the ambient flow speed. A measurement of the flow speed *vs.* distance downstream of Io has been used to show that the plasma returns to approximately corotation speed within <10 R_{Io} (Hinson *et al.* 1998). The speed was inferred by tracking *Galileo*'s radio signal through the region downstream of Io to two different ground receiving stations and determining the time delay for a density anomaly to move from one to another line of sight. A puzzle remains because the theoretical analysis of the distance over which a slowed plasma wake can be re-accelerated to corotation (Southwood and Dunlop 1984) is many times longer. The observation of an extended region of auroral emissions in the jovian ionosphere at locations that map to Io's orbit well downstream of Io's position gives good reason

to believe that the reacceleration of plasma requires more than a few R_{Io}, but the inconsistency with the radio wave measurements remains unexplained.

21.5.2 Europa: Evidence for an Inductive Field

Europa is a very different world from Io. Its icy surface lacks significant relief and there are few craters. No volcanoes are present to serve as the source of heavy ions. Expectations that this body would reveal interesting plasma effects were low prior to *Galileo*'s first encounters, but plasma interactions of considerable interest are found in the vicinity of Europa.

The interaction is in some ways a scaled-down version of the interactions observed at Io. The field magnitude increases upstream of Europa, consistent with slowing of the flow and increasing pickup (Kivelson *et al.* 1999). The Alfvén wing currents produce field bendback (Volwerk *et al.* 1998) indicating the presence of currents that link to the jovian ionosphere. Whistler waves and other plasma waves arise from the non-thermal distributions of plasma in Europa's vicinity (Kurth *et al.* 2001). In the wake region, plasma waves typically associated with current-carrying regions are observed (Kurth *et al.* 2001) and there is also evidence of pickup ions (Paterson *et al.* 1999). Atomic oxygen has been observed in the atmosphere of Europa (Hall *et al.* 1995, 1998), but as O^+ is an important component of the background plasma, this species does not produce the telltale signal in the spectrum of ion cyclotron waves. There are, however, emissions near the ion cyclotron frequency of chlorine (with polarization that suggests the presence of both positive and negative ions), a possible trace pickup ion (Volwerk *et al.* 2001) and weak signals at the gyrofrequency of O_2^+. McNutt (1993) interpreted a signature with mass per unit charge of 19 as doubly ionized potassium, but H_3O^+, easily derived from the surface of Europa by sputtering, ionization, and ion–atom interchange, is also a possible candidate (A. Eviatar, personal communication, 2002). Decreases in the count rates of energetic ions in the region downstream of Europa have been used to examine ion sources and to estimate the speed of the flow approaching Europa (Paranicas *et al.* 2000).

The wake signature in both the energetic particle fluxes and the magnetometer data extends across a region of roughly an Europa diameter, but is not symmetric around the flow direction, a situation that has led simulators to speculate on large radial flows (Kabin *et al.* 1999), but this interpretation has not been supported by measurements.

A dipolar magnetic perturbation was observed in the magnetic field data from *Galileo*'s initial pass by Europa (Kivelson *et al.* 1997b) and the possibility of an inductive response (Neubauer 1999a) seemed probable. After additional passes had occurred, it became possible to establish that the magnetic moment changes sign in phase with the changing sign of the radial field of the magnetosphere, an observation that provided compelling evidence of the presence of a global scale conducting shell capable of carrying substantial electrical currents and located within ~100 km of the surface (Khurana *et al.* 1998, Kivelson *et al.* 1999, 2000, Zimmer *et al.* 2000, Schilling *et al.* 2004). Volwerk *et al.* (1998) reported that the symmetry of the Alfvén wings, with offsets in the radial direction toward/away from Jupiter, appear generally consistent with asymmetries for an induced magnetic response illustrated schematically in Figure 21.3.

The inductive magnetic moment consistent with measurements is of the order of the maximum inductive response for a conducting sphere of radius 1 R_E The work of Zimmer *et al.* (2000) sets bounds on the characteristics of the current carrying layer that can produce the magnetic signature observed. It must lie close to the surface, because the strength of a measured signal decreases with the cube of the ratio of the radius of the conducting shell to the distance from the center of the moon. The magnitude of the inferred magnetic moment places constraints on a combination of the conductivity and the thickness of the shell, but the analysis shows that if the conducting shell has the conductivity of terrestrial seawater, the shell needs to be ~10 km or more in thickness.

The presence of an electrically conducting shell within the icy outer layer of Europa provides insight into the state of the icy material. The electrical conductivity of water ice well below its melting temperature is not large enough to provide the observed inductive response. With increasing temperature, the ice becomes soft and its conductivity rises rapidly as the temperature approaches the melting temperature. There are good reasons to expect temperature to increase with depth because the mantle is a heat source fueled by radioactive decay. Models of the heat flow (Spohn and Schubert 2003) show that for reasonable assumptions regarding the temperature and pressure dependence of the viscosity, it is possible to account for a region of melt below the surface ice, and the characteristics of the icy surface make the presence of a subsurface layer of melt most plausible (Carr *et al.* 1998, Pappalardo *et al.* 1999) although the evidence is not unambiguous (Pappalardo *et al.* 1998, Geissler *et al.* 1998). Because the existence of liquid water is viewed as a desirable, if not necessary, property of a life-supporting environment, there is great interest in seeking further evidence that could establish unambiguously if such a layer is present and how deeply buried it is (Kargel *et al.* 2000).

Evidence in plasma wave measurements for interactions between the jovian magnetosphere and Europa is given by Gurnett *et al.* (1998) and Kurth *et al.* (2001). While the individual observations are quite complex and confused by possible background plasma wave modes that naturally occur near the magnetic equator at Europa's orbit, an approximate picture of this interaction is emerging. As shown in Figure 21.5, electron cyclotron harmonic emissions, usually near $3f_{ce}/2$ with $f_{ce} = eB/2\pi m_e$ the electron cyclotron frequency, are often seen upstream of Europa at distances of 2–3 R_E. A band of whistler-mode emission with bandwidth of ~2 kHz centered near 3 kHz is often seen within an R_E or so of the surface, except in the downstream region. At the closest distances the upper hybrid resonance band is often enhanced, sometimes extending into the downstream wake region. Finally, electrostatic solitary structures are consistently observed in the wake and flux tube of Europa. The modified magnetic field, enhancements in the electron density near the moon due to its plasma source, and anisotropies in the electron distribution function introduced by losses and sources at Europa are likely contributors to the whistler-mode band and electrostatic cyclotron harmonic emissions. The electrostatic solitary structures appear to be very sim-

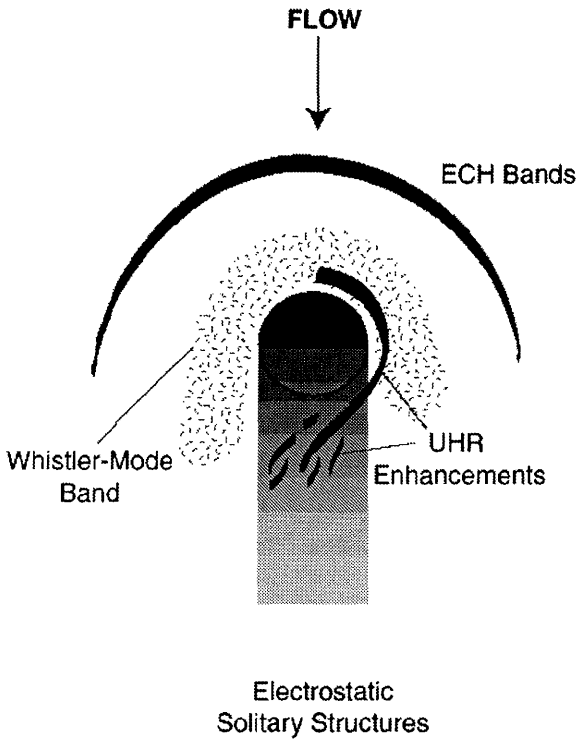

Figure 21.5. Schematic of the distribution of different types of plasma waves in the region around Europa (from Kurth *et al.* 2001).

ilar to those observed at Earth on auroral field lines and in the plasma sheet boundary layer, all places where beams and currents are expected to flow. Hence, it is reasonable to assume that currents flowing between Europa and the jovian ionosphere are ultimately the source of these solitary structures.

21.5.3 Ganymede: Properties of a Mini-Magnetosphere

The discovery of the magnetic field of Ganymede with surface field magnitude as large as 15 times the field of Jupiter's magnetosphere near the moon's orbit (Kivelson *et al.* 1997a,c) has opened new vistas for planetary studies. Prior to *Galileo*'s encounters with Ganymede, it was not even clear that the interior had fully differentiated to form a metallic core, a silicate mantle, and an icy outer layer. The gravitational measurements show that the body has differentiated and does have a metallic core, although the precise size of the core depends on assumptions regarding its composition (Anderson *et al.* 1996). The existence of a substantial magnetic moment appears to indicate that a portion of the central core is fluid and convecting (Schubert *et al.* 1996). The thermal history consistent with a present-day fluid interior is not clearly established, it being unclear just when the internal differentiation occurred and whether it required some contributions from orbital evolution and associated tidal heating (Malhotra 1991, Showman *et al.* 1997, Spohn and Breuer 1998).

Figure 21.6 shows the fields and particles data measured on *Galileo*'s lowest altitude pass over the polar cap of Ganymede (G2). Shown are the plasma wave spectra [see Gurnett *et al.* (1996a) for similar spectra from the G1 pass], the magnetometer measurements (Kivelson *et al.* 1998), the thermal plasma moments (Frank *et al.* 1997a) and the fluxes of energetic particles [see Williams *et al.* (1998) for similar data]. The most striking element of the magnetometer data is the ratio of the amplitude of the field measured at closest approach (~200 km altitude at high latitude) to the background field. Diamonds show the field that would be measured along the orbit if the magnetospheric background field (obtained from the Khurana (1997) field model) were added to a Ganymede-centered dipole field of equatorial magnitude 719 nT, tilted 176° relative to the spin axis. Clearly this is a good approximation to the measured field over most of the pass. The measured B_x component is consistently more negative than the model, a discrepancy attributed to the bending back of the northern Alfvén wing. The sharp rotations at 18:40 and 19:20 UT have been identified as magnetopause crossings and a plot on an expanded scale (top right) reveals the sharp reversals of sign of this component of the field. The magnetopause stands well above the surface of the moon (at an equatorial distance roughly twice the radius of Ganymede). Thus the magnetosphere is one of the smallest known (comparable in size with Mercury's magnetosphere) and the only magnetosphere within a magnetosphere.

The signature of Ganymede's magnetosphere in the plasma wave data is equally clear. In the dynamic spectrum plotted in Figure 21.6, the broadband noise at the magnetopause crossings is evident. Within the magnetosphere, the high frequency cut-off of the lower frequency power ramps up and down in proportion to the field strength at roughly half the electron gyrofrequency in the locally measured magnetic field. Other features typical of waves in a magnetosphere have been identified.

The energetic particle flux, also plotted in Figure 21.6, reveals various important features of the magnetosphere. Anisotropies of ion fluxes related to the plasma flow velocity are present before (after) the inbound (outbound) magnetopause crossing. This is similar to the situation at Earth's dayside magnetopause, where the magnetosheath plasma flows on one side but flow is slow or absent on the other and fluxes are larger when the detector looks into an oncoming flow. The modulation of the data within the magnetopause occurs because as the spacecraft rotates, the EPD instrument samples a range of pitch angles. The strong dips correspond to pitch angles that are in the downward-looking loss cone and reveal the loss of particles that enter Ganymede's polar cap. The size of the loss cones inferred from the angular range of the dips in the flux is consistent with the inferred magnetic field magnitude. The dips are absent outside the magnetopause surface, consistent with being on flux tubes not linked to Ganymede. Fluxes on closed Ganymede field lines are smaller than on field lines that emerge from the polar cap, consistent with expectations for energetic particle responses in the inferred magnetic geometry.

The plasma moments show that the heavy ions of the torus are largely excluded from the Ganymede magnetosphere whereas ions from Ganymede's ionosphere are flowing outward across the polar cap. The outflowing ions were identified as protons in the initial analysis (Frank *et al.* 1997b) but Eviatar and co-workers (Vasyliunas and Eviatar 2000,

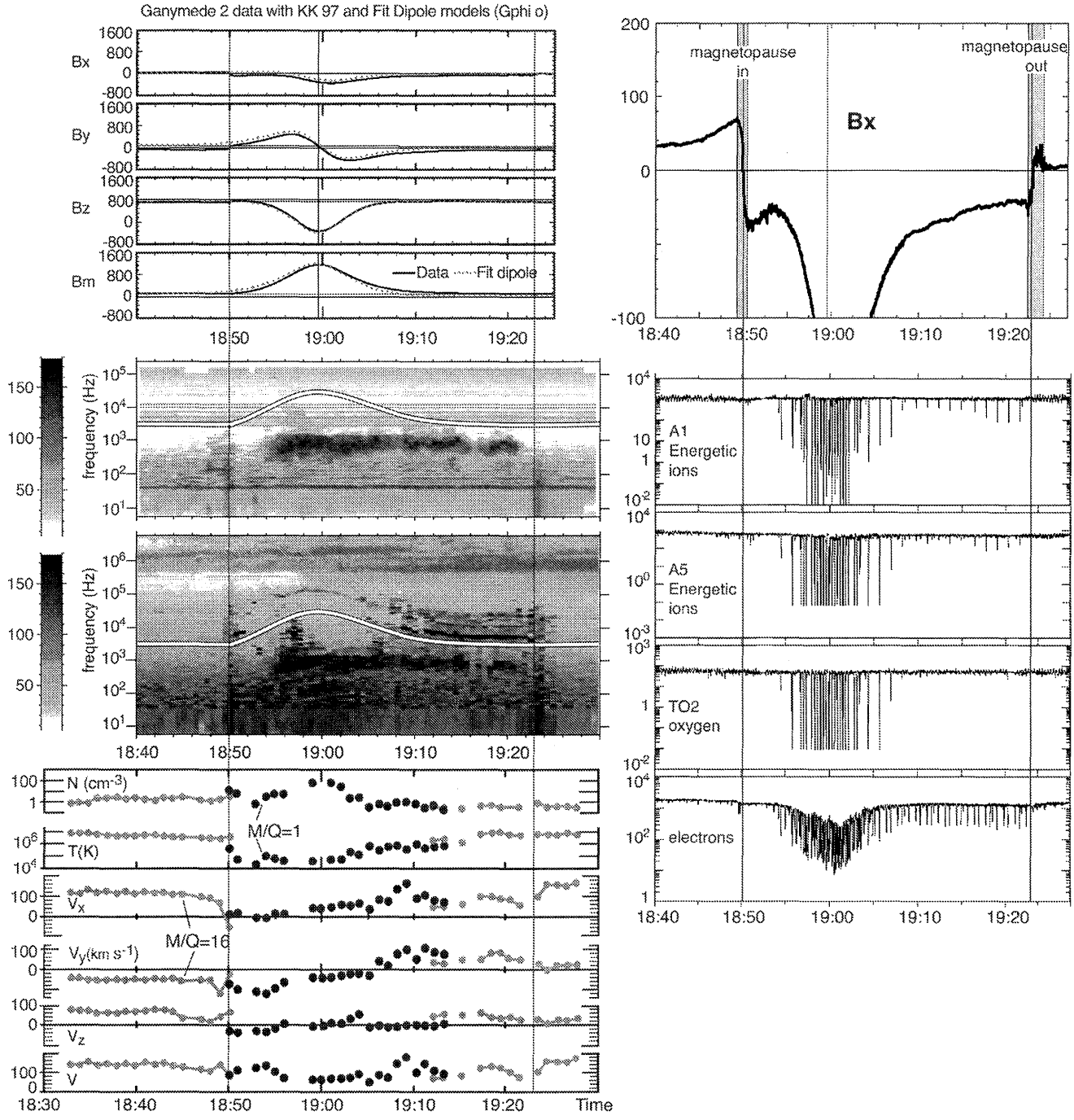

Figure 21.6. Fields and particles data for the G2 flyby of Ganymede, September 6, 1996. Upper left: The magnetic field magnitude (MAG: Kivelson *et al.* 1992) and three components of the field in a Ganymede-centered coordinate system with x along the flow direction, y radially in towards Jupiter, and z along the spin axis. The background field expected in Ganymede's absence is plotted and dots show predictions from a centered internal dipole moment (see text). Middle left: Plasma wave spectra (PWS: Gurnett *et al.* 1992) with electric field dynamic spectra (frequency *vs.* UT) below and magnetic field spectra above. The electron cyclotron frequency based on magnetometer measurements is superimposed in white. Bottom left: Measured proton (black dots) and heavy ion (gray dotted trace) moments (number density, temperature, and flow velocity) (PLS: Frank *et al.* 1992). Top right: A blow-up of the B_x component from which the location of the field rotations were identified. Bottom right: Energetic particle fluxes in counts s^{-1}. Panels from top to bottom are channels A1 and A5, which respond to low-energy ions (predominantly protons, helium, oxygen, and sulfur), TO2, a time of flight channel that measures oxygen flux, and F3 that responds to electrons (EPD: Williams *et al.* 1992). Locations of magnetopause crossings have been superimposed.

Eviatar *et al.* 2001b) demonstrate that the outflowing ions are not protons but ions of atomic oxygen. In either case, there appears to be a polar wind with a source in the polar cap of Ganymede.

The energetic particles that plow into the polar cap sputter neutrals from the surface at a rate that may be as high as 2×10^{26} water molecules s^{-1} (Paranicas *et al.* 1999) leading to an erosion rate of up to 8 m Gyr^{-1}. It is also likely that the energetic particles lost into the polar regions modify the form of the ice crystals and that this is responsible for the observation of changes in the reflectance spectra between polar and low latitude regions. The boundary between the two types of spectral response has been found to correspond quite closely to the boundary between open and closed field lines (illustrated in Figure 21.4) (Khurana, personal communication). Ultraviolet measurements show an absorber, possibly ozone trapped in the ice, in the polar regions in which the energetic charged particles are lost (Hendrix *et al.* 1999). The aurora at Ganymede (Eviatar *et al.* 2001a) also trends along the open–closed field line boundary and reaches the lowest latitude on the downstream side (M. A. McGrath, personal communication, 2001), as in the schematic of Figure 21.4. The close coupling between the structure of Ganymede's magnetosphere and the properties of the atmosphere and surface are beautifully evident in these selected examples of observations.

Ganymede's magnetosphere has not yet been fully analyzed, but analogues to properties familiar from studies of planetary magnetospheres have been reported. Not only, as at Earth and Jupiter, is there an aurora and a startling array of plasma waves as already noted, there are also MHD resonances corresponding to waves standing on closed field lines (Volwerk *et al.* 1999), convective flow on closed field lines (Eviatar *et al.* 1998), a polar wind (Frank *et al.* 1997a, Vasyliunas and Eviatar 2000, Eviatar *et al.* 2001b), and undoubtedly other phenomena not yet reported. One type of magnetospheric response that we do not anticipate at Ganymede is a substorm. The steady, slowly rocking orientation of the magnetic field external to the magnetosphere is expected to drive steady, not bursty, reconnection. This is an issue that still must be investigated and its exploration may cast light on the substorm process at Earth.

Ganymede's interior structure most probably consists of a metallic inner core with radius between 0.33 and 0.5 of its radius, a rocky mantle, and an outer layer of ice roughly 800 km in depth (Anderson *et al.* 1996, 1998b). Recent reanalysis of the magnetic signatures of all the passes near Ganymede indicate that the internal magnetic moment, dominated by a permanent dipole moment probably generated by dynamo action in a deep metallic core, rocks slightly in antiphase with the changing direction of Jupiter's magnetic field. The time-variation arises from an inductive response whose magnitude requires that the induced currents flow in a near-surface conducting shell. It seems likely that Ganymede, like the other icy moons has a layer of melt within ~200 km of the surface and that this layer is sandwiched between layers of ice (Kivelson *et al.* 2002).

Each of *Galileo*'s encounters with Ganymede's magnetosphere has shown a rich plasma wave spectrum, including a significant subset of wave modes expected to be found within any planetary magnetosphere (Gurnett *et al.* 1996a, Kurth *et al.* 1997). At the magnetopause, broadband bursts of electrostatic noise, entirely analogous to similar emissions at the terrestrial magnetopause, are observed. The underlying waveforms indicate the presence of electrostatic solitary structures. The interior of the magnetosphere is dominated by whistler mode hiss and chorus at frequencies below both the electron cyclotron and plasma frequencies and by electron cyclotron harmonic emissions from just above the electron cyclotron frequency to the upper hybrid resonance frequency (f_{uh}). In some cases, the latter band is distinct enough to use as a measure of the electron density (using $n_{\mathrm{e}}(\mathrm{cm}^{-3}) = (f_{\mathrm{uh}}^2 - f_{\mathrm{ce}}^2)/8980^2$). Gurnett *et al.* (1996a) used this information to derive a maximum plasma density along *Galileo*'s trajectory for the first Ganymede flyby of about 45 cm^{-3}. They also provide a density profile that suggests a scale height of about 1000 km and a peak density near the surface of about 100 cm^{-3}. Eviatar *et al.* (2001b) have investigated the Ganymede ionosphere further and "conclude that Ganymede has a bound ionosphere composed mainly of molecular oxygen ions in the polar regions and of atomic oxygen ions at low latitudes." They find a scale height of 600 km and a surface density of about 400 cm^{-3}. The latter is well below the upper limit (inferred from a null observation and the known sensitivity of the detection system) obtained via radio occultation (4×10^3 cm^{-3}) (Kliore 1998). Gurnett *et al.* (1996a) suggest that the whistler mode waves observed during the first passage through a region of "open" field lines (field lines that connect Ganymede and Jupiter) are generated via a loss-cone distribution in electrons with resonant energies of about 150 keV. They also note that anisotropies in lower energy electrons, typically 10–100 eV, are likely the drivers of the electron cyclotron harmonic emissions. Finally Gurnett *et al.* (1996a) and Kurth *et al.* (1997) show that Ganymede's magnetosphere is the source of narrow-band radio emissions in the frequency range of 15–50 kHz, which are thought to be generated via mode conversion from the electrostatic upper hybrid waves into the electromagnetic mode, much as continuum radiation is produced in Earth's magnetosphere.

21.5.4 Callisto: Similarities to Europa and Differences

Callisto lacks a permanent internal magnetic field (Khurana 1997) but like Europa manifests an inductive response to the changing external field of Jupiter's magnetosphere and interacts with the plasma of Jupiter's magnetosphere to form an Alfvén wing (Kivelson *et al.* 1999) much like that illustrated in Figure 21.3. The presence of an Alfvén wing implies that there are conducting paths to close the current system in the surroundings of Callisto, revealing the existence of a thin neutral atmosphere which provides additional plasma and the needed conductivity by pickup. Magnetic fluctuations within the Alfvén wing suggest that the plasma pickup is non-uniform across the surface.

Callisto is only partially differentiated (Anderson *et al.* 1997, 1998a), and has a surface that appears to have been little modified over recent geological time. Thus, it was something of a surprise to find evidence of an inductive field that appears to require sufficient internal heat to produce a layer of melt within the ice (Kivelson *et al.* 1999, Zimmer *et al.* 2000). Recent reconsideration of the heat flow models show that by modeling the interior convection using stress depen-

dent viscosity that varies with temperature and pressure, the cooling of the interior is reduced (Spohn and Schubert 2003, Ruiz 2001, Bennett 2001) and it is possible to understand the presence of an ocean layer surrounded by ice both below and above.

Of all the Galilean satellites, Callisto exhibits the least significant interaction with its environment based on evidence from plasma wave observations (Gurnett *et al.* 1998, 2000). The only signatures reported to date are broadband bursty emissions extending upwards from the lowest frequencies and upper hybrid resonance emissions observed on only two of the flybys. The bursty emissions could either be electrostatic solitary waves or kinetic Alfvén waves. The upper hybrid bands are likely produced in response to newly ionized plasma from a source on Callisto, although such a plasma source is only sporadically seen. Two possibilities may explain this. First, it is possible, as suggested by Gurnett *et al.* (2000), that the ionosphere is bound very close to Callisto and only very close flybys allow an *in situ* observer to measure it. Alternatively, the neutral source varies in time and extends down the wake of the satellite only under certain conditions. Gurnett *et al.* (2000) point out that solar illumination may play a role in determining the nature of the plasma in the wake. This would be consistent with the report (Kliore *et al.* 2001) of a strong correlation between the detection of an ionosphere at Callisto and the times when the sub-ram and subsolar longitudes are similar, that is when the Sun illuminates the trailing hemisphere.

21.6 SUMMARY AND OUTSTANDING QUESTIONS

The physical processes revealed in the regions of space surrounding the Galilean moons are remarkably diverse and in many cases were unexpected. Today we can describe many features of the interaction with an extended ionosphere and comet-like features that dominate the surroundings of Io, understand the nature of the magnetospheric interaction region discovered at Ganymede, and model the Alfvénic responses of the moons Europa and Callisto with their induced magnetic moments. Many uncertainties remain, and their elucidation will no doubt show that there are further uncertainties.

We are, for example, still uncertain about the mechanism that produces excitations at the feet of the flux tubes linked to Io, Europa, and Ganymede. Particle beams observed in the near wake region of Io may be the source of the excitations or may merely be responses to field-aligned electric fields at low altitudes that generate the beams observed at Io. The wake region that leads Io in its orbit links to a latitudinally narrow tail of emission in the jovian ionosphere, suggesting a role for field-aligned currents that must flow to reaccelerate the plasma of the wake region. On the other hand, measurements of flow velocities in Io's wake suggest that the slowing ends within less than 10 Io radii, so some other explanation of the extended ionospheric tail may be relevant.

In considering Ganymede's magnetosphere as a possible example of steady reconnection, details of the distribution of accelerated particles and modified flows have not been explored and should be investigated both in data and in simulations. Those flows must take the magnetic flux over the polar cap, but there must be a closure region downstream of Ganymede and the properties of the return flow remain poorly described.

For Europa, the response to the changing magnetic field has been found consistent with the presence of a conducting shell embedded within the icy surface layers, but neither the depth nor the thickness of the conducting layer has been established. Measurements from a spacecraft in orbit around Europa have been under consideration in recent years, and measurements of the inductive response to both the diurnal and orbital variability of the magnetic field could place constraints on both the depth and the thickness of the current-carrying layer.

More immediately, there will be data on yet another large moon embedded in a planetary magnetosphere from the *Cassini* measurements at Titan. Table 21.1 gives the key parameters of the Titan interaction. Most critical is the importance of mass pickup, which implies that among the Galilean moons, Io, with its extended ionosphere, provides the closest parallel. On the other hand the table suggests that the dynamics are dominated by plasma pressure instead of the magnetic field pressure in contrast to Io. Hence the flow is super-Alfvénic but subsonic, yielding a fast Mach number <1 in agreement with the lack of observations of a bow shock during the *Voyager 1* encounter (Ness *et al.* 1982, Gurnett *et al.* 1981). Most of the other dimensionless parameters that characterize the interaction fall outside the range that has been encountered for the Galilean moons. One can anticipate that the exploration of Titan and its plasma environment will greatly enrich our knowledge of the modes of electromagnetic interactions with planet scale bodies.

In summary, the following outstanding questions remain:

- What are the physical mechanisms that produce auroral emissions at the base of the flux tubes linked to Io, Europa, and Ganymede?
- What is the nature of the plasma flow associated with Ganymede's magnetosphere? Is Ganymede's magnetosphere an example of steady reconnection?
- At Europa, what is the depth and thickness of a possible conducting layer within the icy surface layers?
- How does the plasma interaction at Titan compare with that of the Galilean satellites?

Acknowledgements. The authors thank Peter Delamere for converting the chapter to Latex. MGK acknowledges support by the National Science Foundation under ATM-02-05958 and by NASA under JPL 1238965. FB acknowledges support by NASA under JPL 959550.

REFERENCES

Acuna, M. H., F. M. Neubauer, and N. F. Ness, Standing Alfvén wave current system at Io: *Voyager 1* observations, *J. Geophys. Res.* **86**, 8513–8521, 1981.

Acuna, M. H., K. W. Behannon, and J. E. P. Connerney, Jupiter's magnetic field and magnetosphere, in *Physics of the jovian Magnetosphere*, A. J. Dessler (ed.), pp. 1–50, 1983.

Anderson, J. D., E. L. Lau, W. L. Sjogren, G. Schubert, and W. B. Moore, Gravitational constraints on the internal structure of Ganymede, *Nature* **384**, 541–543, 1996.

Anderson, J. D., E. L. Lau, W. L. Sjogren, G. Schubert, and W. B. Moore, Gravitational evidence for an undifferentiated Callisto, *Nature* **387**, 264–266, 1997.

Anderson, J. D., G. Schubert, R. A. Jacobson, E. L. Lau, W. B. Moore, and W. L. Sjo Gren, Distribution of rock, metals, and ices in Callisto, *Science* **280**, 1573, 1998a.

Anderson, J. D., G. Schubert, R. A. Jacobson, E. L. Lau, W. B. Moore, and W. L. Sjo Gren, Structure: Inferences from four *Galileo* encounters, *Science* **281**, 2019, 1998b.

Bagenal, F., Empirical model of the Io plasma torus: *Voyager* measurements, *J. Geophys. Res.* **99**, 11 043–11 062, 1994.

Bagenal, F. and Y. Leblanc, Io's Alfvén wave pattern and the jovian decametric arcs, *A&A* **197**, 311–319, 1988.

Bagenal, F., D. E. Shemansky, R. L. McNutt, R. Schreier, and A. Eviatar, The abundance of O^{2+} in the jovian magnetosphere, *Geophys. Res. Lett.* **19**, 79–82, 1992.

Bagenal, F., F. J. Crary, A. I. F. Stewart, N. M. Schneider, D. A. Gurnett, W. S. Kurth, L. A. Frank, and W. R. Paterson, *Galileo* measurements of plasma density in the Io torus, *Geophys. Res. Lett.* **24**, 2119, 1997.

Barbosa, D. D., On the injection and scattering of protons in Jupiter's magnetosphere, *J. Geophys. Res.* **86**, 8981–8990, 1981.

Belcher, J. W., C. K. Goertz, J. D. Sullivan, and M. H. Acuna, Plasma observations of the Alfvén wave generated by Io, *J. Geophys. Res.* **86**, 8508–8512, 1981.

Bennett, K. A., Planetary science: Uncool Callisto, *Nature* **412**, 395–396, 2001.

Bigg, E. K., Influence of the satellite Io on Jupiter's decametric emission, *Nature* **203**, 1008–1010, 1964.

Brown, M. E., Observation of mass loading in the Io plasma torus, *Geophys. Res. Lett.* **21**, 847–850, 1994.

Brown, R. A., Optical line emission from Io, in *Exploration of the Planetary System*, vol. 65, pp. 527–531, 1974.

Brown, R. A., C. B. Pilcher, and D. F. Strobel, Spectrophotometric Studies of the Io Torus, in *Physics of the jovian Magnetosphere*, A. J. Dessler (ed.), pp. 197–225, 1983.

Burger, M. H., N. M. Schneider, and J. K. Wilson, *Galileo*'s close-up view of the Io sodium jet, *Geophys. Res. Lett.* **26**, 3333, 1999.

Carlson, R. W., A tenuous carbon dioxide atmosphere on Jupiter's moon Callisto, *Science* **283**, 820, 1999.

Carr, M. H., M. J. S. Belton, C. R. Chapman, M. E. Davies, P. Geissler, R. Greenberg, A. S. McEwen, B. R. Tufts, R. Greeley, and R. Sullivan, Evidence for a subsurface ocean on Europa, *Nature* **391**, 363, 1998.

Carr, T. D., M. D. Desch, and J. K. Alexander, Phenomenology of magnetospheric radio emissions, in *Physics of the Jovian Magnetosphere*, A.J. Dessler (ed.), pp. 226–284, 1983.

Cheng, A. F. and C. Paranicas, Model of field-aligned potential drops near Io, *Geophys. Res. Lett.* **25**, 833, 1998.

Chust, T., A. Roux, S. Perraut, P. Louarn, W. S. Kurth, and D. A. Gurnett, *Galileo* plasma wave observations of iogenic hydrogen, *Planet. Space Sci.* **47**, 1377–1387, 1999.

Clarke, J. T., G. E. Ballester, J. Trauger, R. Evans, J. E. P. Connerney, K. Stapelfeldt, D. Crisp, P. D. Feldman, C. J. Burrows, S. Casertano, J. S. Gallagher, R. E. Griffiths, J. J. Hester, J. G. Hoessel, J. A. Holtzman, J. E. Krist, V. Meadows, J. R. Mould, P. A. Scowen, A. M. Watson, and J. A. Westphal, Far-ultraviolet imaging of Jupiter's aurora and the Io "Footprint", *Science* **274**, 404–409, 1996.

Clarke, J. T., G. Ballester, J. Trauger, J. Ajello, W. Pryor, K. Tobiska, J. E. P. Connerney, G. R. Gladstone, J. H. Waite, L. Ben Jaffel, and J. Gérard, Hubble Space Telescope imaging of Jupiter's UV aurora during the *Galileo* orbiter mission, *J. Geophys. Res.* **103**, 20 217–20 236, 1998.

Combi, M. R., K. Kabin, T. I. Gombosi, D. L. Dezeeuw, and K. G. Powell, Io's plasma environment during the *Galileo* flyby: Global three-dimensional MHD modeling with adaptive mesh refinement, *J. Geophys. Res.* **103**, 9071–9082, 1998.

Combi, M. R., T. I. Gombosi, and K.Kabin, Plasma flow past cometary and planetary satellite atmospheres, in *Atmospheres in the Solar System: Comparative Aeronomy*, M. Mendillo, A. Nagy, J. H. Waite (eds), AGU, pp. 151–167, 2002.

Connerney, J. E. P., R. Baron, T. Satoh, and T. Owen, Images of excited H_3^+ at the foot of the Io flux tube in Jupiter's atmosphere, *Science* **262**, 1035–1038, 1993.

Cooper, J. F., R. E. Johnson, B. H. Mauk, H. B. Garrett, and N. Gehrels, Energetic ion and electron irradiation of the icy Galilean satellites, *Icarus* **149**, 133–159, 2001.

Crary, F. J. and F. Bagenal, Coupling the plasma interaction at Io to Jupiter, *Geophys. Res. Lett.* **24**, 2135, 1997.

Crary, F. J., F. Bagenal, L. A. Frank, and W. R. Paterson, *Galileo* plasma spectrometer measurements of composition and temperature in the Io plasma torus, *J. Geophys. Res.* **103**, 29 359–29 370, 1998.

Cummings, A. C. and E. C. Stone, Anomalous cosmic rays and solar modulation, *Space Sci. Rev.* **83**, 51–62, 1998.

de Pater, I., F. Marchis, H. Roe, B. Macintosh, S. Acton, D. Le Mignant, and W. M. Keck, Jupiter I (Io), *IAU Circ.* **7588**, 2, 2001.

Delamere, P., F. Bagenal, R. Ergun, and Y. Su, Momentum transfer between the Io plasma wake and Jupiter's magnetosphere, *J. Geophys. Res.*, **108**, 1241, 2003.

Drell, S. D., H. M. Foley, and M. A. Ruderman, Drag and propulsion of large satellites in the ionosphere: An Alfvén propulsion engine in space, *J. Geophys. Res.* **70**, 3131, 1965.

Eviatar, A., A. F. Cheng, C. Paranicas, B. H. Mauk, R. W. McEntire, and D. J. Williams, Plasma flow in the magnetosphere of Ganymede, *Geophys. Res. Lett.* **25**, 1257, 1998.

Eviatar, A., D. F. Strobel, B. C. Wolven, P. D. Feldman, M. A. McGrath, and D. J. Williams, Excitation of the Ganymede ultraviolet aurora, *ApJ* **555**, 1013–1019, 2001a.

Eviatar, A., V. M. Vasyliūnas, and D. A. Gurnett, The ionosphere of Ganymede, *Planet. Space Sci.* **49**, 327–336, 2001b.

Feldman, P. D., M. A. McGrath, D. F. Strobel, H. W. Moos, K. D. Retherford, and B. C. Wolven, HST/STIS ultraviolet imaging of polar aurora on Ganymede, *ApJ* **535**, 1085–1090, 2000.

Frank, L. A. and W. R. Paterson, Intense electron beams observed at Io with the *Galileo* spacecraft, *J. Geophys. Res.* **104**, 28 657, 1999a.

Frank, L. A. and W. R. Paterson, Production of hydrogen ions at Io, *J. Geophys. Res.* **104**, 10 345–10 354, 1999b.

Frank, L. A. and W. R. Paterson, Return to Io by the *Galileo* spacecraft: Plasma observations, *J. Geophys. Res.* **105**, 25 363–25 378, 2000.

Frank, L. A. and W. R. Paterson, Passage through Io's ionospheric plasmas by the *Galileo* spacecraft, *J. Geophys. Res.* **106**, 26 209–26 224, 2001a.

Frank, L. A. and W. R. Paterson, Survey of thermal ions in the Io plasma torus with the *Galileo* spacecraft, *J. Geophys. Res.* **106**, 6131–6150, 2001b.

Frank, L. A., K. L. Ackerson, J. A. Lee, M. R. English, and G. L. Pickett, The plasma instrumentation for the *Galileo* mission, *Space Sci. Rev.* **60**, 283, 1992.

Frank, L. A., W. R. Paterson, K. L. Ackerson, V. M. Vasyliunas, F. V. Coroniti, and S. J. Bolton, Plasma observations at Io with the *Galileo* spacecraft, *Science* **274**, 394–395, 1996.

Frank, L. A., W. R. Paterson, K. L. Ackerson, and S. J. Bolton, Low-energy electron measurements at Ganymede with the *Galileo* spacecraft: Probes of the magnetic topology, *Geophys. Res. Lett.* **24**, 2159, 1997a.

Frank, L. A., W. R. Paterson, K. L. Ackerson, and S. J. Bolton, Outflow of hydrogen ions from Ganymede, *Geophys. Res. Lett.* **24**, 2151, 1997b.

Geissler, P. E., R. Greenberg, G. Hoppa, P. Helfenstein, A. McEwen, R. Pappalardo, R. Tufts, M. Ockert-Bell, R. Sullivan, and R. Greeley, Evidence for non-synchronous rotation of Europa, *Nature* **391**, 368, 1998.

Glatzmaier, G. A., P. J. Tackley, M. G. Kivelson, W. B. Moore, P. H. Roberts, and G. Schubert, Numerical simulations of magnetoconvection in the core of Io, *Eos* pp. 11B–05, 1998.

Goertz, C. K., Io's interaction with the plasma torus, *J. Geophys. Res.* **85**, 2949–2956, 1980.

Goertz, C. K. and P. A. Deift, Io's interaction with the magnetosphere, *Planet. Space Sci.* **21**, 1399–1415, 1973.

Goldreich, P. and D. Lynden-Bell, Io, a jovian unipolar inductor, *ApJ* **156**, 59–78, 1969.

Gurnett, D. A. and C. K. Goertz, Multiple Alfvén wave reflections excited by Io: Origin of the jovian decametric arcs, *J. Geophys. Res.* **86**, 717–722, 1981.

Gurnett, D. A., W. S. Kurth, and F. L. Scarf, Plasma waves near Saturn: Initial results from *Voyager 1*, *Science* **212**, 235–239, 1981.

Gurnett, D. A., W. S. Kurth, R. R. Shaw, A. Roux, R. Gendrin, C. F. Kennel, F. L. Scarf, and S. D. Shawhan, The *Galileo* plasma wave investigation, *Space Sci. Rev.* **60**, 341–355, 1992.

Gurnett, D. A., W. S. Kurth, A. Roux, S. J. Bolton, and C. F. Kennel, Evidence for a magnetosphere at Ganymede from the plasma-wave observations by the *Galileo* spacecraft, *Nature* **384**, 535–537, 1996a.

Gurnett, D. A., W. S. Kurth, A. Roux, S. J. Bolton, and C. F. Kennel, *Galileo* plasma wave observations in the Io plasma torus and near Io, *Science* **274**, 391–392, 1996b.

Gurnett, D. A., W. S. Kurth, A. Roux, S. J. Bolton, E. A. Thomsen, and J. B. Groene, *Galileo* plasma wave observations near Europa, *Geophys. Res. Lett.* **25**, 237, 1998.

Gurnett, D. A., A. M. Persoon, W. S. Kurth, A. Roux, and S. J. Bolton, Plasma densities in the vicinity of Callisto from *Galileo* plasma wave observations, *Geophys. Res. Lett.* **27**, 1867, 2000.

Gurnett, D. A., A. M. Persoon, W. S. Kurth, A. Roux, and S. J. Bolton, Electron densities near Io from *Galileo* plasma wave observations, *J. Geophys. Res.* **106**, 26 225–26 232, 2001.

Hall, D. T., D. F. Strobel, P. D. Feldman, M. A. McGrath, and H. A. Weaver, Detection of an oxygen atmosphere on Jupiter's moon Europa, *Nature* **373**, 677, 1995.

Hall, D. T., P. D. Feldman, M. A. McGrath, and D. F. Strobel, The far-ultraviolet oxygen airglow of Europa and Ganymede, *ApJ* **499**, 475, 1998.

Hartle, R. E., E. C. Sittler, K. W. Ogilvie, J. D. Scudder, A. J. Lazarus, and S. K. Atreya, Titan's ion exosphere observed from *Voyager 1*, *J. Geophys. Res.* **87**, 1383–1394, 1982.

Hendrix, A. R., C. A. Barth, and C. W. Hord, Ganymede's ozone-like absorber: Observations by the *Galileo* ultraviolet spectrometer, *J. Geophys. Res.* **104**, 14 169–14 178, 1999.

Hill, T. W. and D. H. Pontius, Plasma injection near Io, *J. Geophys. Res.* **103**, 19 879–19 886, 1998.

Hill, T. W., and V. M. Vasyliunas, Jovian auroral signature of Io's corotational wake, *J. Geophys. Res.*, **107**, 1464, 2002.

Hill, T. W., A. J. Dessler, and C. K. Goertz, Configuration of the jovian magnetosphere, *Geophys. Res. Lett.* **1**, 3, 1974.

Hill, T. W., A. J. Dessler, and C. K. Goertz, Magnetospheric models, in *Physics of the Jovian Magnetosphere*, A. J. Dessler (ed.), pp. 353–394, 1983.

Hinson, D. P., A. J. Kliore, F. M. Flasar, J. D. Twicken, P. J. Schinder, and R. G. Herrera, *Galileo* radio occultation measurements of Io's ionosphere and plasma wake, *J. Geophys. Res.* **103**, 29 343–29 357, 1998.

Huddleston, D. E., R. J. Strangeway, J. Warnecke, C. T. Russell, M. G. Kivelson, and F. Bagenal, Ion cyclotron waves in the Io torus during the *Galileo* encounter: Warm plasma dispersion analysis, *Geophys. Res. Lett.* **24**, 2143, 1997.

Intriligator, D. S. and W. D. Miller, First evidence for a Europa plasma torus, *J. Geophys. Res.* **87**, 8081–8090, 1982.

Ip, W.-H., D. J. Williams, R. W. McEntire, and B. H. Mauk, Ion sputtering and surface erosion at Europa, *Geophys. Res. Lett.* **25**, 829, 1998.

Johnson, R. E., *Energetic Charged-Particle Interactions with Atmospheres and Surfaces*, Springer-Verlag, 1990.

Joy, S. P., M. G. Kivelson, R. J. Walker, K. K. Khurana, C. T. Russell, and T. Ogino, Probabilistic models of the jovian magnetosphere and bow shock locations, *J. Geophys. Res.* **107**, 17–1, 2002.

Kabin, K., M. R. Combi, T. I. Gombosi, A. F. Nagy, D. L. Dezeeuw, and K. G. Powell, On Europa's magnetospheric interaction: A MHD simulation of the E4 flyby, *J. Geophys. Res.* **104**, 19 983–19 992, 1999.

Kabin, K., M. R. Combi, T. I. Gombosi, D. L. DeZeeuw, K. C. Hansen, and K. G. Powell, Io's magnetospheric interaction: An MHD model with day–night asymmetry, *Planet. Space Sci.* **49**, 337–344, 2001.

Kane, M., D. J. Williams, B. H. Mauk, R. W. McEntire, and E. C. Roelof, *Galileo* energetic particles detector measurements of hot ions in the neutral sheet region of Jupiter's magnetodisk, *Geophys. Res. Lett.* **26**, 5, 1999.

Kargel, J. S., J. Z. Kaye, J. W. Head, G. M. Marion, R. Sassen, J. K. Crowley, O. P. Ballesteros, S. A. Grant, and D. L. Hogenboom, Europa's crust and ocean: Origin, composition, and the prospects for life, *Icarus* **148**, 226–265, 2000.

Khurana, K. K., Euler potential models of Jupiter's magnetospheric field, *J. Geophys. Res.* **102**, 11 295–11 306, 1997.

Khurana, K. K., Influence of solar wind on Jupiter's magnetosphere deduced from currents in the equatorial plane, *J. Geophys. Res.* **106**, 25 999–26 016, 2001.

Khurana, K. K., M. G. Kivelson, D. J. Stevenson, G. Schubert, C. T. Russell, R. J. Walker, S. Joy, and C. Polansky, Induced magnetic fields as evidence for subsurface oceans in Europa and Callisto, *Nature* **395**, 777, 1998.

Khurana, K. K., M. G. Kivelson, C. T. Russel, R. J. Walker, and S. Joy, Io's magnetic field, *European Geophys. U.* , 2002.

Kivelson, M. G., Pulsations and magnetohydrodynamic waves, in *Introduction to Space Physics*, M. G. Kivelson and C. T. Russell (eds), pp. 330–355, Cambridge University Press, 1995.

Kivelson, M. G., J. A. Slavin, and D. J. Southwood, Magnetospheres of the Galilean satellites, *Science* **205**, 491–493, 1979.

Kivelson, M. G., K. K. Khurana, J. D. Means, C. T. Russell, and R. C. Snare, The *Galileo* magnetic field investigation, *Space Sci. Rev.* **60**, 357–383, 1992.

Kivelson, M. G., K. K. Khurana, R. J. Walker, J. A. Linker, C. R. Russell, D. J. Southwood, and C. Polanskey, A magnetic signature at Io: Initial report from the *Galileo* magnetometer, *Science* **273**, 337–340, 1996a.

Kivelson, M. G., K. K. Khurana, R. J. Walker, J. Warnecke, C. T. Russell, J. A. Linker, D. J. Southwood, and C. Polanskey, Io's interaction with the plasma torus: *Galileo* magnetometer report, *Science* **274**, 396, 1996b.

Kivelson, M. G., K. K. Khurana, F. V. Coroniti, S. Joy, C. T. Russell, R. J. Walker, J. Warnecke, L. Bennett, and C. Polanskey, Magnetic field and magnetosphere of Ganymede, *Geophys. Res. Lett.* **24**, 2155, 1997a.

Kivelson, M. G., K. K. Khurana, S. Joy, C. T. Russell, R. J. Walker, and C. Polansky, Europa's magnetic signature: Report from *Galileo*'s first pass on December 19, 1996, *Science* **276**, 1239, 1997b.

Kivelson, M. G., K. K. Khurana, C. T. Russell, R. J. Walker, P. J. Coleman, F. V. Coroniti, J. Green, S. Joy, R. L. McPherron, and C. Polanskey, *Galileo* at Jupiter: Changing states of the magnetosphere and first looks at Io and Ganymede, *Adv. Space Res.* **20**, 193, 1997c.

Kivelson, M. G., J. Warnecke, L. Bennett, S. Jóy, K. K. Khurana, J. A. Linker, C. T. Russell, R. J. Walker, and C. Polanskey, Ganymede's magnetosphere: Magnetometer overview, *J. Geophys. Res.* **103**, 19 963–19 972, 1998.

Kivelson, M. G., K. K. Khurana, D. J. Stevenson, L. Bennett, S. Joy, C. T. Russell, R. J. Walker, C. Zimmer, and C. Polanskey, Europa and Callisto: Induced or intrinsic fields in a periodically varying plasma environment, *J. Geophys. Res.* **104**, 4609–4626, 1999.

Kivelson, M. G., K. K. Khurana, C. T. Russell, M. Volwerk, R. J. Walker, and C. Zimmer, *Galileo* magnetometer measurements: A stronger case for a subsurface ocean at Europa, *Science* **289**, 1340–1343, 2000.

Kivelson, M. G., K. K. Khurana, C. T. Russell, S. P. Joy, M. Volwerk, R. J. Walker, C. Zimmer, and J. A. Linker, Magnetized or unmagnetized: Ambiguity persists following *Galileo*'s encounters with Io in 1999 and 2000, *J. Geophys. Res.* **106**, 26 121–26 136, 2001a.

Kivelson, M. G., K. K. Khurana, C. T. Russell, and R. J. Walker, Magnetic signature of a polar pass over Io, *Eos* pp. 11A–01, 2001b.

Kivelson, M. G., K. K. Khurana, and M. Volwerk, The permanent and inductive magnetic moments of Ganymede, *Icarus* **157**, 507–522, 2002.

Kliore, A. J., Satellite atmospheres and magnetospheres, *Highlights in Astronomy* **11**, 1065, 1998.

Kliore, A. J., A. Anabtawi, and A. F. Nagy, The ionosphere of Callisto observed by *Galileo* radio science, *BAAS* **32**, 0, 2000.

Kliore, A. J., A. Anabtawi, and A. F. Nagy, The ionospheres of Europa, Ganymede, and Callisto, *Eos* p. B506, 2001.

Krupp, N., A. Lagg, S. Livi, B. Wilken, J. Woch, E. C. Roelof, and D. J. Williams, Global flows of energetic ions in Jupiter's equatorial plane: First-order approximation, *J. Geophys. Res.* **106**, 26 017–26 032, 2001.

Kurth, W. S., D. A. Gurnett, A. Roux, and S. J. Bolton, Ganymede: A new radio source, *Geophys. Res. Lett.* **24**, 2167, 1997.

Kurth, W. S., D. A. Gurnett, A. M. Persoon, A. Roux, S. J. Bolton, and C. J. Alexander, The plasma wave environment of Europa, *Planet. Space Sci.* **49**, 345–363, 2001.

Leblanc, Y., G. A. Dulk, and F. Bagenal, On Io's excitation and the origin of Jupiter's decametric radiation, *A&A* **290**, 660–673, 1994.

Lellouch, E., T. Encrenaz, M. Belton, I. de Pater, and S. Gulkis, Io's atmosphere from microwave detection SO_2, *Nature* **346**, 639–641, 1990.

Linker, J. A., M. G. Kivelson, and R. J. Walker, An MHD simulation of plasma flow past Io: Alfvén and slow mode perturbations, *Geophys. Res. Lett.* **15**, 1311–1314, 1988.

Linker, J. A., M. G. Kivelson, and R. J. Walker, A three-dimensional MHD simulation of plasma flow past Io, *J. Geophys. Res.* **96**, 21 037, 1991.

Linker, J. A., K. K. Khurana, M. G. Kivelson, and R. J. Walker, MHD simulations of Io's interaction with the plasma torus, *J. Geophys. Res.* **103**, 19 867–19 878, 1998.

Linker, J. A., M. G. Kivelson, R. J. Walker, and M. A. McGrath, Io's magnetic and plasma environment: What can be learned from the I24 and I25 flybys?, *Eos* **80**, F621, 1999.

Liu, Y., A. F. Nagy, K. Kabin, M. R. Combi, D. L. Dezeeuw, T. I. Gombosi, and K. G. Powell, Two-species, 3D, MHD simulation of Europa's interaction with Jupiter's magnetosphere, *Geophys. Res. Lett.* **27**, 1791, 2000.

Lopes-Gautier, R., S. Douté, W. D. Smythe, L. W. Kamp, R. W. Carlson, A. G. Davies, F. E. Leader, A. S. McEwen, P. E. Geissler, S. W. Kieffer, L. Keszthelyi, E. Barbinis, R. Mehlman, M. Segura, J. Shirley, and L. A. Soderblom, A close-up look at Io from *Galileo*'s Near Infrared Mapping Spectrometer, *Science* **288**, 1201–1204, 2000.

Luhmann, J. G., Plasma interactions with unmagnetized bodies, in *Introduction to Space Physics*, M. G. Kivelson and C. T. Russell (eds), pp. 203–226, Cambridge University Press, 1995.

Malhotra, R., Tidal origin of the Laplace resonance and the resurfacing of Ganymede, *Icarus* **94**, 399–412, 1991.

Mauk, B. H., S. A. Gary, M. Kane, E. P. Keath, S. M. Krimigis, and T. P. Armstrong, Hot plasma parameters of Jupiter's inner magnetosphere, *J. Geophys. Res.* **101**, 7685–7696, 1996.

Mauk, B. H., R. W. McEntire, D. J. Williams, A. Lagg, E. C. Roelof, S. M. Krimigis, T. P. Armstrong, T. A. Fritz, L. J. Lanzerotti, and J. G. Roederer, *Galileo*-measured depletion of near-Io hot ring current plasmas since the *Voyager* epoch, *J. Geophys. Res.* **103**, 4715, 1998.

McNutt, R. L., Possible in situ detection of K(2+) in the jovian magnetosphere, *J. Geophys. Res.* **98**, 21 221, 1993.

McNutt, R. L., J. W. Belcher, and H. S. Bridge, Positive ion observations in the middle magnetosphere of Jupiter, *J. Geophys. Res.* **86**, 8319, 1981.

Mead, G. D. and W. N. Hess, Jupiter's radiation belt and the sweeping effect of its satellites, *J. Geophys. Res.* **78**, 2793–2811, 1973.

Mekler, Y. and A. Eviatar, Spectroscopic observations of Io, *ApJ* **193**, L151, 1974.

Mendillo, M., J. Baumgardner, B. Flynn, and W. J. Hughes, The extended sodium nebula of Jupiter, *Nature* **348**, 312–314, 1990.

Mendillo, M., B. Flynn, and J. Baumgardner, Imaging observations of Jupiter's sodium magneto-nebula during the ULYSSES encounter, *Science* **257**, 1510–1512, 1992.

Menietti, J. D., D. A. Gurnett, W. S. Kurth, and J. B. Groene, Control of jovian radio emission by Ganymede, *Geophys. Res. Lett.* **25**, 4281, 1998.

Menietti, J. D., D. A. Gurnett, and I. Christopher, Control of jovian radio emission by Callisto, *Geophys. Res. Lett.* **28**, 3047, 2001.

Morabito, L. A., S. P. Synnott, P. N. Kupferman, and S. A. Collins, Discovery of currently active extraterrestrial volcanism, *Science* **204**, 972, 1979.

Morrison, D. and J. Samz, *Voyage to Jupiter*, NASA, 1980.

Ness, N. F., M. H. Acuna, R. P. Lepping, J. E. P. Connerney, K. W. Behannon, L. F. Burlaga, and F. M. Neubauer, Magnetic field studies by *Voyager 1*: Preliminary results at Saturn, *Science* **212**, 211–217, 1981.

Ness, N. F., M. H. Acuna, and K. W. Behannon, The induced magnetosphere of Titan, *J. Geophys. Res.* **87**, 1369–1381, 1982.

Neubauer, F. M., Possible strengths of dynamo magnetic fields of the Galilean satellites and of Titan, *Geophys. Res. Lett.* **5**, 905–908, 1978.

Neubauer, F. M., Nonlinear standing Alfvén wave current system at Io: Theory, *J. Geophys. Res.* **85**, 1171–1178, 1980.

Neubauer, F. M., Comment on "Interaction of Io with its torus: Does Io have an internal magnetic field?" by Khurana, Kivelson and Russell, *Geophys. Res. Lett.* **25**, 2349, 1998a.

Neubauer, F. M., The sub-Alfvénic interaction of the Galilean satellites with the jovian magnetosphere, *J. Geophys. Res.* **103**, 19 843–19 866, 1998b.

Neubauer, F. M., Alfvén wings and electromagnetic induction in the interiors: Europa and Callisto, *J. Geophys. Res.* **104**, 28 671, 1999a.

Neubauer, F. M., Erratum: "The sub-Alfvénic interaction of the Galilean satellites with the jovian magnetosphere, *J. Geophys. Res.* **104**, 3863–3864, 1999b.

Neubauer, F. M., On the plasma distribution in the polar regions of the Galilean satellites, particularly Io: Field-aligned plasma motion, in *Eos*, 2000.

Oliversen, R. J., F. Scherb, W. H. Smyth, M. E. Freed, R. Carey Woodward, M. L. Marconi, K. D. Retherford, O. L. Lupie, and J. P. Morgenthaler, Sunlit Io atmospheric [O I] 6300 Å emission and the plasma torus, *J. Geophys. Res.* **106**, 26 183–26 194, 2001.

Pappalardo, R. T., J. W. Head, R. Greeley, R. J. Sullivan, C. Pilcher, G. Schubert, W. B. Moore, M. H. Carr, J. M. Moore, and M. J. S. Belton, Geological evidence for solid-state convection in Europa's ice shell, *Nature* **391**, 365, 1998.

Pappalardo, R. T., M. J. S. Belton, H. H. Breneman, M. H. Carr, C. R. Chapman, G. C. Collins, T. Denk, S. Fagents, P. E. Geissler, B. Giese, R. Greeley, R. Greenberg, J. W. Head, P. Helfenstein, G. Hoppa, *et al.*, Does Europa have a subsurface ocean? Evaluation of the geological evidence, *J. Geophys. Res.* **104**, 24 015–24 056, 1999.

Paranicas, C., A. F. Cheng, and D. J. Williams, Inference of Europa's conductance from the *Galileo* Energetic Particles Detector, *J. Geophys. Res.* **103**, 15 001–15 008, 1998.

Paranicas, C., W. R. Paterson, A. F. Cheng, B. H. Mauk, R. W. McEntire, L. A. Frank, and D. J. Williams, Energetic particle observations near Ganymede, *J. Geophys. Res.* **104**, 17 459–17 470, 1999.

Paranicas, C., R. W. McEntire, A. F. Cheng, A. Lagg, and D. J. Williams, Energetic charged particles near Europa, *J. Geophys. Res.* **105**, 16 005–16 016, 2000.

Paranicas, C., R. W. Carlson, and R. E. Johnson, Electron bombardment of Europa, *Geophys. Res. Lett.* **28**, 673, 2001.

Paranicas, C., J. M. Ratliff, B. H. Mauk, C. Cohen, and R. E. Johnson, The ion environment near Europa and its role in surface energetics, *Geophys. Res. Lett.* **29**, 18–1, 2002.

Paterson, W. R., L. A. Frank, and K. L. Ackerson, *Galileo* plasma observations at Europa: Ion energy spectra and moments, *J. Geophys. Res.* **104**, 22 779–22 792, 1999.

Peale, S. J., P. Cassen, and R. T. Reynolds, Melting of Io by tidal dissipation, *Science* **203**, 892–894, 1979.

Piddington, J. H., Electrodynamic effects of Jupiter's satellite Io, *Nature* **217**, 1968.

Richardson, J. D. and G. L. Siscoe, Factors governing the ratio of inward to outward diffusing flux of satellite ions, *J. Geophys. Res.* **86**, 8485–8490, 1981.

Ruiz, J., The stability against freezing of an internal liquid-water ocean in Callisto, *Nature* **412**, 409–411, 2001.

Russell, C. T. and M. G. Kivelson, Detection of SO in Io's exosphere, *Science* **287**, 1998–1999, 2000.

Russell, C. T., M. G. Kivelson, K. K. Khurana, and D. E. Huddleston, Magnetic fluctuations close to Io: Ion cyclotron and mirror mode wave properties, *Planet. Space Sci.* **47**, 143, 1999.

Saur, J., D. F. Strobel, and F. M. Neubauer, Interaction of the jovian magnetosphere with Europa: Constraints on the neutral atmosphere, *J. Geophys. Res.* **103**, 19 947–19 962, 1998.

Saur, J., F. M. Neubauer, D. F. Strobel, and M. E. Summers, Three-dimensional plasma simulation of Io's interaction with the Io plasma torus: Asymmetric plasma flow, *J. Geophys. Res.* **104**, 25 105–25 126, 1999.

Saur, J., F. M. Neubauer, D. F. Strobel, and M. E. Summers, Io's ultraviolet aurora: Remote sensing of Io's interaction, *Geophys. Res. Lett.* **27**, 2893, 2000.

Saur, J., F. M. Neubauer, D. F. Strobel, and M. E. Summers, Interpretation of *Galileo*'s Io plasma and field observations: I0, I24, and I27 flybys and close polar passes, *J. Geophys. Res.* pp. 5–1, 2002.

Schardt, A. W. and C. K. Goertz, High-energy particles, in *Physics of the Jovian Magnetosphere*, A. J. Dessler (ed.), pp. 157–196, 1983.

Scherb, F. and W. H. Smyth, Variability of (O I) 6300-A emission near Io, *J. Geophys. Res.* **98**, 18 729, 1993.

Schilling, N., K. K. Khurana, and M. G. Kivelson, Limits on an intrinsic dipole moment in Europa, *J. Geophys. Res.*, 2004, **in press**.

Schneider, N. M. and J. T. Trauger, The structure of the Io torus, *ApJ* **450**, 450, 1995.

Schreier, R., A. Eviatar, V. M. Vasyliunas, and J. D. Richardson, Modeling the Europa plasma torus, *J. Geophys. Res.* **98**, 21 231, 1993.

Schubert, G., K. Zhang, M. G. Kivelson, and J. D. Anderson, The magnetic field and internal structure of Ganymede, *Nature* **384**, 544–545, 1996.

Scudder, J. D., E. C. Sittler, and H. S. Bridge, A survey of the plasma electron environment of Jupiter: A view from *Voyager*, *J. Geophys. Res.* **86**, 8157–8179, 1981.

Shemansky, D. E. and G. R. Smith, The *Voyager 1* EUV spectrum of the Io plasma torus, *J. Geophys. Res.* **86**, 9179–9192, 1981.

Showman, A. P., D. J. Stevenson, and R. Malhotra, Coupled orbital and thermal evolution of Ganymede, *Icarus* **129**, 367–383, 1997.

Smith, E. J., J. L. Davis, D. E. Jones, J. P. J. Coleman, D. S. Colburn, P. Dyal, C. P. Sonett, and A. M. Frandsen, The planetary magnetic field and magnetosphere of Jupiter: *Pioneer 10*, *J. Geophys. Res.* **79**, 3501, 1974.

Smith, E. J., L. Davis, and D. E. Jones, Jupiter's magnetic field and magnetosphere, in *Jupiter*, T. Gehrels (ed.), University of Arizona Press, pp. 788–829, 1976.

Smyth, W. H., Energy escape rate of neutrals from Io and the implications for local magnetospheric interactions, *J. Geophys. Res.* **103**, 11 941–11 950, 1998.

Smyth, W. H. and M. B. McElroy, The sodium and hydrogen gas clouds of Io, *Planet. Space Sci.* **25**, 415–431, 1977.

Southwood, D. J. and M. W. Dunlop, Mass pickup in sub-Alfvénic plasma flow: A case study for Io, *Planet. Space Sci.* **32**, 1079–1086, 1984.

Southwood, D. J. and A. N. Fazakerley, The interaction of Io with the jovian magnetosphere, *Adv. Space Res.* **12**, 359–365, 1992.

Southwood, D. J. and M. G. Kivelson, A new perspective concerning the influence of the solar wind on the jovian magnetosphere, *J. Geophys. Res.* **106**, 6123–6130, 2001.

Southwood, D. J., M. G. Kivelson, R. J. Walker, and J. A. Slavin, Io and its plasma environment, *J. Geophys. Res.* **85**, 5959–5968, 1980.

Spohn, T. and D. Breuer, Interior structure and evolution of the Galilean satellites, in *Planetary Systems: The Long View*, L. Celnikier and J. T. T. Van (eds), Editions Frontières, pp. 135–144, 1998.

Spohn, T. and G. Schubert, Oceans in the icy Galilean satellites of Jupiter, *Icarus* **161**, 456–467, 2003.

Strobel, D. F. and B. C. Wolven, The atmosphere of Io: Abundances and sources of sulfur dioxide and atomic hydrogen, *Ap&SS* **277**, 271–287, 2001.

Su, Y., R. Ergun, F. Bagenal, and P. Delamere, Io-related auroral arcs: Modelling parallel electric fields, *J. Geophys. Res.*, **108**, 1094, 2003.

Tackley, P. J., G. Schubert, G. A. Glatzmaier, P. Schenk, J. T. Ratcliff, and J.-P. Matas, Three-dimensional simulations of mantle convection in Io, *Icarus* **149**, 79–93, 2001.

Taylor, M. H., N. M. Schneider, F. Bagenal, B. R. Sandel, D. E. Shemansky, P. L. Matheson, and D. T. Hall, A comparison of the *Voyager 1* ultraviolet spectrometer and plasma science measurements of the Io plasma torus, *J. Geophys. Res.* **100**, 19 541–19 550, 1995.

Thomas, N., G. Lichtenberg, and M. Scotto, High-resolution spectroscopy of the Io plasma torus during the *Galileo* mission, *J. Geophys. Res.* **106**, 26 277–26 292, 2001.

Thomsen, M. F., C. K. Goertz, and J. A. van Allen, On determining magnetospheric diffusion coefficients from the observed effects of Jupiter's satellite Io, *J. Geophys. Res.* **82**, 5541–5550, 1977.

Vasyliunas, V. M. and A. Eviatar, Outflow of ions from Ganymede: A reinterpretation, *Geophys. Res. Lett.* **27**, 1347, 2000.

Volwerk, M., M. G. Kivelson, K. K. Khurana, D. E. Huddleston, and R. J. Strangeway, Ion pickup and asymmetries in Europa's wake, *Eos* **79**, F551, 1998.

Volwerk, M., M. G. Kivelson, K. K. Khurana, and R. L. McPherron, Probing Ganymede's magnetosphere with field line resonances, *J. Geophys. Res.* **104**, 14 729–14 738, 1999.

Volwerk, M., M. G. Kivelson, and K. K. Khurana, Wave activity in Europa's wake: Implications for ion pickup, *J. Geophys. Res.* **106**, 26 033–26 048, 2001.

Warnecke, J., M. G. Kivelson, K. K. Khurana, D. E. Huddleston, and C. T. Russell, Ion cyclotron waves observed at *Galileo*'s Io encounter: Implications for neutral cloud distribution and plasma composition, *Geophys. Res. Lett.* **24**, 2139, 1997.

Wienbruch, U. and T. Spohn, A self sustained magnetic field on Io?, *Planet. Space Sci.* **43**, 1045–1057, 1995.

Williams, D., Ganymede's ionic radiation belts, *Geophys. Res. Lett.* , 2001.

Williams, D. J., Energetic particle environment in the jovian magnetosphere, in *Conf. on Magnetospheres of the Outer Planets*, Paris, France, p. 19, 2001.

Williams, D. J., R. W. McEntire, S. Jaskulek, and B. Wilken, The *Galileo* Energetic Particles Detector, *Space Sci. Rev.* **60**, 385–412, 1992.

Williams, D. J., B. H. Mauk, R. E. McEntire, E. C. Roelof, T. P. Armstrong, B. Wilken, J. G. Roederer, S. M. Krimigis, T. A. Fritz, and L. J. Lanzerotti, Electron beams and ion composition measured at Io and in its torus, *Science* **274**, 401, 1996.

Williams, D. J., B. Mauk, and R. W. McEntire, Properties of Ganymede's magnetosphere as revealed by energetic particle observations, *J. Geophys. Res.* **103**, 17 523–17 534, 1998.

Wolf-Gladrow, D. A., F. M. Neubauer, and M. Lussem, Io's interaction with the plasma torus: A self-consistent model, *J. Geophys. Res.* **92**, 9949–9961, 1987.

Woodward, R. C. J., F. Scherb, and F. L. Roesler, Periodic intensity variations in sulfur emissions from the Io plasma torus, *Icarus* **111**, 45–64, 1994.

Wright, A. N. and D. J. Southwood, Stationary Alfvénic structures, *J. Geophys. Res.* **92**, 1167–1175, 1987.

Zimmer, C., K. K. Khurana, and M. G. Kivelson, Subsurface oceans on Europa and Callisto: Constraints from *Galileo* magnetometer observations, *Icarus* **147**, 329–347, 2000.